Volume 28
Number 12
23 March 2026
Pages 5121-5508

Green Chemistry

Cutting-edge research for a greener sustainable future

rsc.li/greenchem

ISSN 1463-9262

ROYAL SOCIETY OF CHEMISTRY

TUTORIAL REVIEW

Xiaomeng You, Lin Dai, Tong-Qi Yuan *et al.*

Muconic acid: a renewable platform monomer for polymer materials

Green Chemistry

TUTORIAL REVIEW

View Article Online
View Journal | View Issue

Cite this: *Green Chem.*, 2026, **28**, 5167

Muconic acid: a renewable platform monomer for polymer materials

Aocheng Wei,[a,b] Qinyang Lei,[a,b] Xiaomeng You,*[a,b] Xiaojun Shen,[a,b] Lin Dai*[c] and Tong-Qi Yuan*[a,b]

Received 7th January 2026,
Accepted 16th February 2026

DOI: 10.1039/d6gc00103c

rsc.li/greenchem

Future generations of polymers must not only originate from renewable feedstocks but also deliver tailored functionality and be conceived with intrinsic recyclability or environmentally benign end-of-life pathways. Muconic acid (MA), sourcing from abundant lignocellulosic biomass or industrial side streams through state-of-the-art microbial fermentation or chemo-catalytic routes, possesses a distinctive molecular architecture—comprising a conjugated diene alongside two carboxylic acid groups—that renders it a highly adaptable precursor for a broad spectrum of value-added monomers and polymeric materials. MA has a tremendous potential to serve as a renewable building block for conventional polymer families, as well as to enable entirely new green material architectures. While, the journey from sustainable MA production to the realization of commercially viable green materials entails systematic research across the entire value chain—from environmentally benign synthesis and efficient polymerization methodologies, to the properties and applications of the resulting polymers. In this review, the structure, sources, polymerization strategies of MA are described, its applications are assessed, and prospects for the development of advanced MA-based polymers materials are discussed.

Green foundation

1. Muconic acid, sourced from abundant lignocellulosic biomass and industrial side streams through state-of-the-art microbial fermentation or chemo-catalytic routes, is garnering increasing recognition as a renewable building block for both established polymer families and novel, high-performance material architectures.
2. The journey from sustainable muconic acid production to the realization of commercially viable, circular materials entails navigating complex scientific and technological challenges. Hence, the review advances green chemistry by connecting the sustainable production of muconic acid to its polymerization into advanced materials.
3. By showcasing the potential of malonic acid as a renewable feedstock for polymer materials, the insights from this review highlight opportunities to meat advanced emerging demand by gene editing, metabolic engineering, and precise control of polymer structure.

1. Introduction

Petroleum polymers are extensively utilized in industrial and civilian applications owing to their robust performance and versatility. However, their synthesis process relies primarily on non-renewable fossil resources, and their waste products are not easily degraded, which greatly restricts the development of sustainable strategies. The widespread use of these materials not only accelerates the depletion of petroleum reserves but also introduces persistent pollutants into ecosystems. Furthermore, the polymer manufacturing process emits greenhouse gases and toxic byproducts, exacerbating climate change and environmental degradation.[1–4] In this context, the production of bio-based polymers using renewable biomass resources to liberate ourselves from our dependence on petroleum and move ever closer to bio-based materials finds widespread support as a common vision among materials scientists around the world. This vision is of great relevance for fossil resource consumption, environmental pollution reduction, and the circular economy.[5–9]

Muconic acid (MA) stands as a remarkable compound, which has evolved from an ancient research object into a pivotal bio-based platform compound with significant modern value. In 1909, the German chemist M. Jaffé first reported muconic acid as a urinary metabolite in rabbits and dogs after

[a]*State Key Laboratory of Efficient Production of Forest Resources, Beijing Forestry University, Beijing 100083, China. E-mail: xiaomengyou@bjfu.edu.cn, ytq581234@bjfu.edu.cn*
[b]*Beijing Key Laboratory of Lignocellulosic Chemistry, Beijing Forestry University, Beijing 100083, China*
[c]*State Key Laboratory of Biobased Fiber Materials, Tianjin Key Laboratory of Pulp and Paper, College of Light Industry and Engineering, Tianjin University of Science and Technology, Tianjin 300457, China. E-mail: dailin@tust.edu.cn*

benzene administration.[10] Following more than a century of dedicated research, it can now be produced at scale *via* tailored chemical routes and engineered biological pathways. Chemical conversion methods utilize petroleum-based aromatic compounds as feedstock and rely on metal catalysts for oxidative cracking. This approach not only faces limitations imposed by fossil resources but also suffers from drawbacks such as difficult product purification and severe pollution. In contrast, the biotechnological fermentation method utilizes renewable resources such as glucose, lignin derivatives, and industrial waste. By engineering metabolic pathways in bacteria like *Escherichia coli* or fungi like *Bacillus thuringiensis*, this approach offers significant advantages, including environmental friendliness, resource renewability, and high product purity.[11–14]

The intrinsic value of MA, irrespective of its origin *via* natural discovery or artificial synthesis through chemical and biological pathways, is fundamentally rooted in its distinctive molecular architecture: a straight-chain dicarboxylic acid featuring a conjugated diene system. This specific structure endows it with exceptional utility as a versatile platform chemical, serving as a key precursor for the synthesis of high-value bulk commodities, most notably adipic acid—a critical monomer in nylon production.[15–17] MA can be used to perform polycondensation with carboxyl groups to create polyesters, polyamides through carboxyl condensation polymerization,[18–23] but also can be used for addition polymerization through double bonds,[24–28] or coordination polymerization with metal cations.[29–34] In addition, muconate derivative also has potential for topological polymerization.[24,35–37] Consistent with the "bioprivileged molecules" paradigm, MA has been highlighted as a representative biomass-derived intermediate that can be diversified into both drop-in replacements and novel molecules with enhanced end-use performance.[8,38] At present, the main use of MA is to hydrogenate it to obtain adipic acid (precursor of nylon-6,6) and terephthalic acid (precursor of PET) through Diels–Alder addition.[15–17,39–41] These multi-stage conversion processes consume extra energy and provide no atom-economy advantage. Therefore, strategies to directly utilize MA are currently being developed.

The inherent structural tunability of MA serves as the foundation for engineering polymers with diverse functional properties and broad application potential. This versatility is exemplified through distinct polymerization pathways: polycondensation reactions generate unsaturated polymers featuring reactive conjugated backbones, which are amenable to post-polymerization modification;[18,20,22,23] addition (or topological) polymerization yields highly stereoregular architectures;[24,35–37,42–64] and coordination polymerization facilitates the construction of three-dimensional metal–organic frameworks (MOFs) with promising utility in catalysis, sensing, and energy technologies.[29–31] Recent years have witnessed substantial progress in the field, marked by optimized biosynthesis of MA, innovative design of its functional derivatives, and the development of advanced polymerization techniques. These collective efforts have significantly accelerated the integration of MA-based materials into high-performance polymers, functional MOFs, and next-generation energy materials. Nonetheless, the translation of this potential into widespread commercial reality is constrained by persistent challenges, including high production costs, intricate synthesis processes, and limited yields, which represent critical bottlenecks demanding innovative solutions.

This review presents a chemistry-centred perspective on the evolving landscape of MA-based polymers, with the aim of systematically deciphering the intricate interplay between molecular structure, synthetic methodology, material property, and ultimate function. We commence by establishing a robust chemical foundation, encompassing the stereochemistry, electronic properties, and reactivity profiles of key MA isomers and their strategically designed derivatives. A critical evaluation of their production—contrasting precision chemical synthesis with metabolic pathway engineering—sets the stage for subsequent discussions on polymerizability. The core of this review mechanistically unpacks the major polymerization including polycondensation, addition polymerization, and coordination polymerization. This structure-centric analysis naturally transitions to a survey of emergent applications, where specific chemical features of MA-derived polymers are connected to their performance in the domains of structural, environmental, energy, electronic, and other materials. Ultimately, we provide a forward-looking analysis that identifies persistent chemical and engineering challenges—such as monomer purity, catalytic efficiency, and scalability of complex syntheses—and proposes targeted research directions to overcome them (Fig. 1). By framing MA not merely as a monomer but as a versatile chemical platform, this review is intended to inspire innovative synthetic strategies and foster the rational design of the next generation of sustainable, high-performance polymeric materials.

2. Muconic acid: an overview

2.1 Muconic acid structures and derivatives

The presence of conjugated double bonds in MA gives rise to distinct isomers with significantly divergent physicochemical properties. In addition, MA has a high melting point and low solubility in usual solvents; thus, it is not easily used directly for polymer synthesis and usually converted into other materials, such as diesters or ammonium salts, and then polymerized (Fig. 2). Thus, it is important to know the properties of MA and its derivatives to use them for polymer synthesis.

2.1.1 Muconic acid isomers. Muconic acid exists as three stereoisomers: *cis*,*cis*-muconic acid (ccMA), *cis*,*trans*-muconic acid (ctMA), and *trans*,*trans*-muconic acid (ttMA). Their differences originate from the spatial configuration of the pair of conjugated double bonds. Different double bond geometries lead to variations in physical properties, synthesis routes, and application potential.

cis,*cis*-Muconic acid (ccMA) is one of the three MA isomers, first identified in its ester form in 1923 *via* debromination of

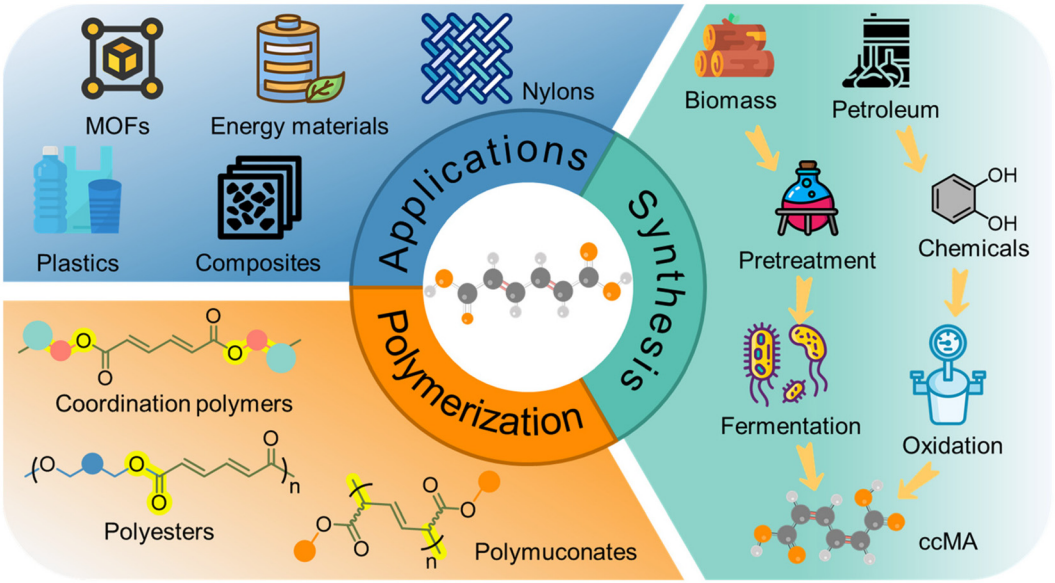

Fig. 1 Synthesis of MA and polymerization pathways and applications of MA-based polymers.

dimethyl 3,4-dibromoadipate with pyridine.[65] In ccMA, both double bonds are in the *cis* configuration, meaning the functional groups (carboxyl and the other C=C bond) on each side of the double bond are on the same side, resulting in a relatively closed overall structure. It has a melting point of approximately 195 °C,[66] a pK_a of 3.57,[67] low water solubility (~1 g L^{-1}),[68] and moderate solubility in organic solvents (*e.g.*, ~0.168 mol mol^{-1} in ethanol).[66] It readily undergoes lactonization, especially under acidic conditions, forming muconolactone.[69] ccMA is the primary product obtained from biological fermentation. Its main current application is hydrogenation to adipic acid, the precursor for nylon-6,6, with very high conversion rates.[15–17,39,41,70] ccMA also typically serves as the precursor for the other isomers, convertible *via* isomerization reactions.[71–74]

The *cis*,*cis* and *cis*,*trans* isomers of muconic acid show significant similarity. After the identification of the *cis*,*cis* isomer, the existence of the *cis*,*trans* isomer remained unrecognized.[75] Following extensive research on MA synthesis, Elvidge *et al.* successfully provided the first definitive identification of the ctMA isomer. In ctMA, one double bond is *cis* and the other is *trans*. It has a melting point of ~190 °C,[76] a pK_a of 2.9, solubility in water(~5.2 g L^{-1}),[77] and solubility in organic solvents is higher than ccMA, making purification easier.[11] Under acidic conditions, it can further isomerize to ttMA or undergo lactonization. It is primarily generated by spontaneous isomerization of ccMA under acidic conditions; for example, at pH 5.1, ccMA can convert to 85% ctMA.[78] In microbial fermentation broths, *in situ* isomerization can be induced by pH adjustment, simplifying the separation process.[79,80]

trans,*trans*-Muconic acid (ttMA) has both double bonds in the *trans* configuration, resulting in a linear overall structure, and is the thermodynamically most stable isomer. It has a high melting point of ~301 °C,[81] a pK_a of 3.4, very low water solubility (<0.1 g L^{-1}), and low solubility in organic solvents.[11] It does not readily undergo lactonization and exhibits high chemical stability. The high melting point and low solubility of ttMA, distinct from the other two isomers, stem from the rigid *trans* double bond configuration enabling tighter molecular packing in the crystal lattice, stronger intermolecular forces (*e.g.*, van der Waals, hydrogen bonding), and thus a more stable crystal structure requiring higher energy to disrupt.[82] It cannot be synthesized directly by microorganisms and must be obtained *via* chemical conversion or isomerization. MA possesses a pair of conjugated double bonds, granting it potential for Diels–Alder (DA) reactions.[83] However, the steric effects of the *cis*,*cis* and *cis*,*trans* isomers hinder their participation in DA reactions. Consequently, ttMA is widely used for DA additions, with its primary application focused on the production of terephthalic acid.[41]

Additionally, there is *trans*-β-hydromuconic acid (HA), which can be obtained from renewable resources *via* electrocatalytic hydrogenation after glucose fermentation. HA contains only one double bond. Well-defined polyesters can be prepared *via* polycondensation without isomerization or C=C bond saturation, owing to the highly stable non-conjugated C=C bond in HA.[19,68]

2.1.2 Muconic acid derivatives. The carboxylic acid groups in MA are strongly electron-withdrawing, reducing the electron density of the double bonds. This makes direct free radical polymerization difficult, as the carboxyl groups diminish the monomer's reactivity towards radical intermediates, hindering radical propagation. Additionally, in acidic media, the carboxyl groups can protonate, and the ionized form experiences significant electrostatic repulsion with radicals, leading to a marked decrease in chain propagation rates. Therefore, for

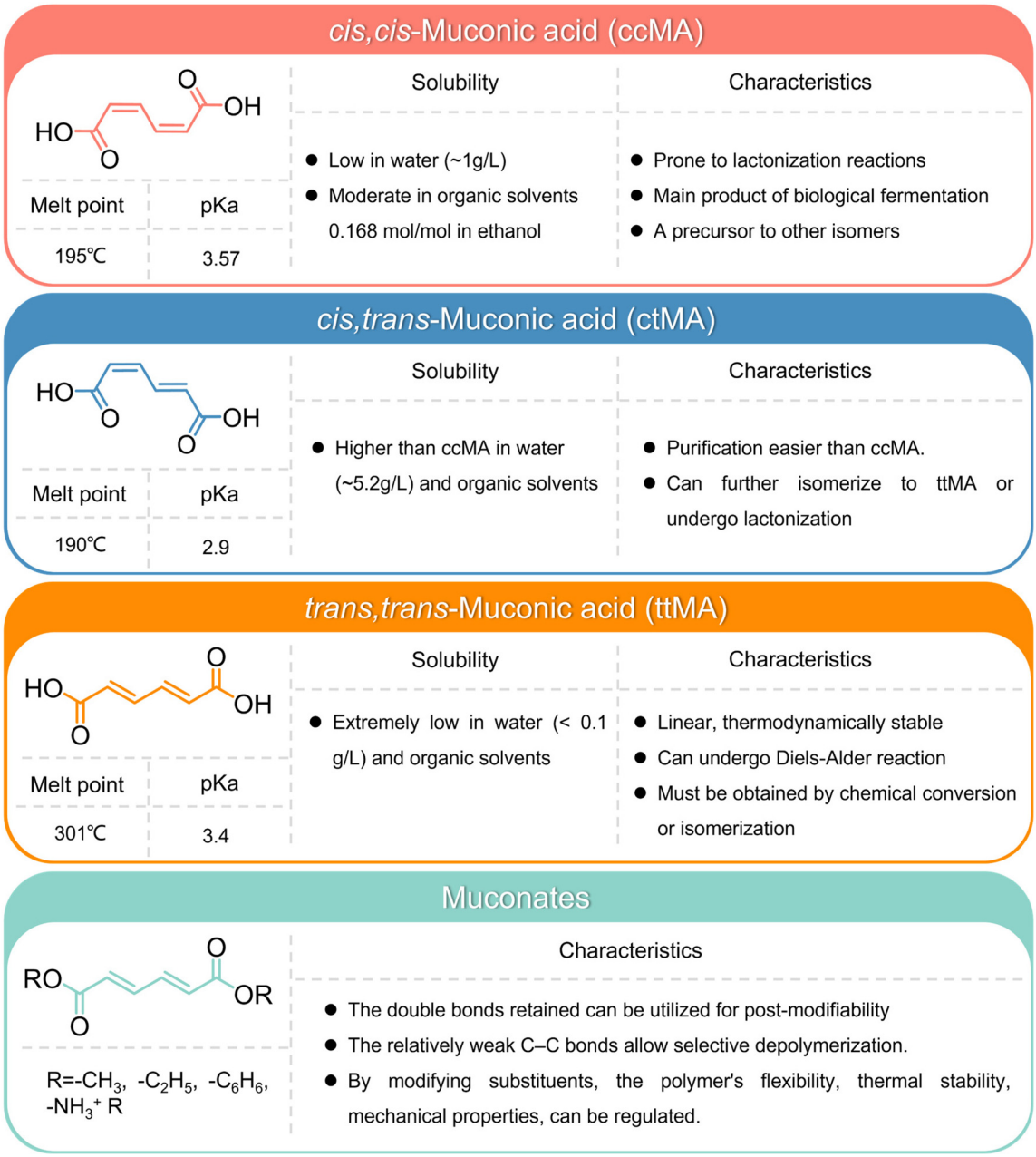

Fig. 2 The physical properties and characteristics of the three isomers of MA and their derivatives.

polymerization involving the double bonds, MA is often derivatized *via* esterification to form corresponding muconate esters (*e.g.*, alkyl esters, benzyl esters, alkoxybenzyl esters) or converted to ammonium salts.

The unique crystal properties of MA derivatives grant them potential for topochemical polymerization, which offers extremely high stereoselectivity but is highly sensitive to molecular structure.[45] In 1999, Matsumoto *et al.* reported that X-ray analysis of diethyl (*Z*,*Z*)-muconate (EMU) crystals revealed molecules arranged in a columnar stack, with the diene parts stacked face-to-face, and the distance between double bonds (~3.79 Å) falling within the range required for topochemical polymerization. This stacking was not reliant on hydrogen bonding but achieved stable arrangement through dipole interactions of the ester groups, molecular geometric symmetry, and van der Waals forces.[36] In the crystal structure of EMU, molecules form regular columnar arrays through the steric and electronic effects of the ester groups. Although lacking the 2D hydrogen-bonding network of ammonium salts, this specific packing mode still maintains crystal order, meeting the strict requirements of topochemical polymerization for molecular alignment (*e.g.*, double bond orientation, spacing). Besides esters, primary ammonium carboxylates serve as supramolecular synthons capable of forming robust

hydrogen-bonding networks. Their preparation is straightforward, and they are widely used in studies of chiral recognition and selective reactions in the crystalline state. Thus, MA is also converted to ammonium salt forms to search for monomers capable of topochemical polymerization. Alkylammonium (*Z*,*Z*)-muconates can polymerize in the crystalline state upon light irradiation. Furthermore, the cycle of ammonium-acid conversion can yield similar polymer crystals while maintaining the layered structure and crystal habit.[45]

Moreover, polymers derived from MA possess intrinsically weakened C–C single bonds. The C–C bond lengths in these polymers are significantly longer than those in conventional polymers. Increased bond length reduces orbital overlap between carbon atoms, directly weakening bond energy. This characteristic enables direct, selective depolymerization of MA-based polymers at elevated temperatures without requiring additional reactants or catalysts.[25,28,84]

2.2 Sources of muconic acid

There are two major sources of MA: chemical conversion and biological fermentation (Fig. 3). The chemical method is an old strategy to synthesize MA. Its basic idea is to oxidatively cleave the aromatic rings of fossil-based feedstocks (*e.g.*, phenol and catechol) in the presence of heavy-metal catalysts. The advantages of chemical conversion are well-established, mature technology, and a fast reaction process. When the feedstock is a simple compound such as catechol, MA can be synthesized directly *via* a one-pot oxidation reaction, with a short reaction path. However, heavy metal catalysts used in the chemical method, greenhouse gases generated by chemical reaction, and toxic byproducts also cause serious environmental pollution. As for the chemical method, the risk of fossil resource depletion exists for the selection of petroleum-based feedstocks. Meanwhile, there are many by-products and mixed isomers in the products, and separation and purification will increase costs. It is also challenging to recycle expensive heavy metal catalysts.

The main advantages of biotechnological fermentation come from the fact that it is an environmentally friendly technology, mild reaction conditions lead to fewer pollutants, and there are abundant and renewable biomass resources or waste materials available for selection, which are in line with the development of sustainable environment. In addition, the products are highly pure and can be directly obtain ccMA without a separation process. However, the metabolic pathway of some microorganisms shows low flux, and further metabolic engineering strategy (knockout of competing pathway, overexpression of rate-limiting enzyme) should be used to improve the conversion yield. Moreover, some target substrates (vanillin, catechol) are toxic to microorganisms, and screening of a tolerant strain or optimization of feeding strategy (fed-batch feeding) should be used to deal with them. These processes can only synthesize ccMA, if ctMA and ttMA are needed, chemical isomerization process will be used to increase the process complexity.

2.2.1 Chemical synthesis. The chemical synthesis of MA primarily targets ttMA and ccMA (Fig. 4). The mainstream synthesis uses catechol as the primary starting material, with some attempts using phenol (due to its accessibility and theoretical advantages, despite high direct oxidation difficulty). Reaction systems are complex, employing various oxidants including hydrogen peroxide (H_2O_2), peroxy acids

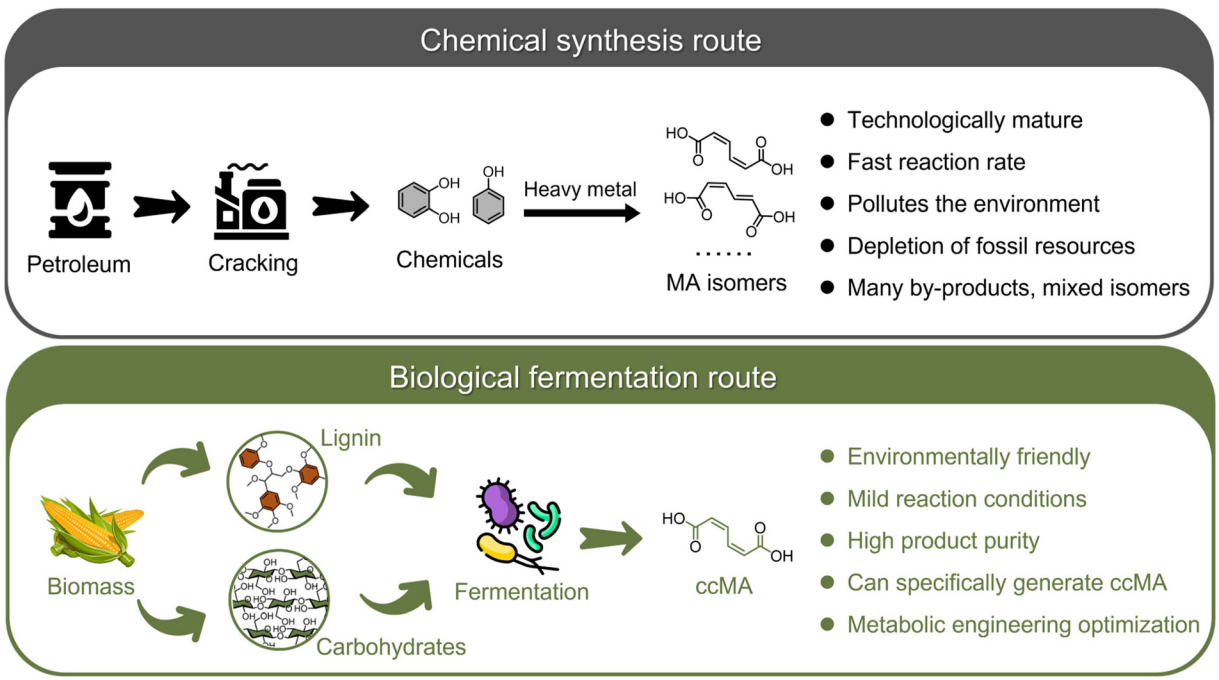

Fig. 3 The chemical synthesis route and biological fermentation route of MA: processes and key characteristics.

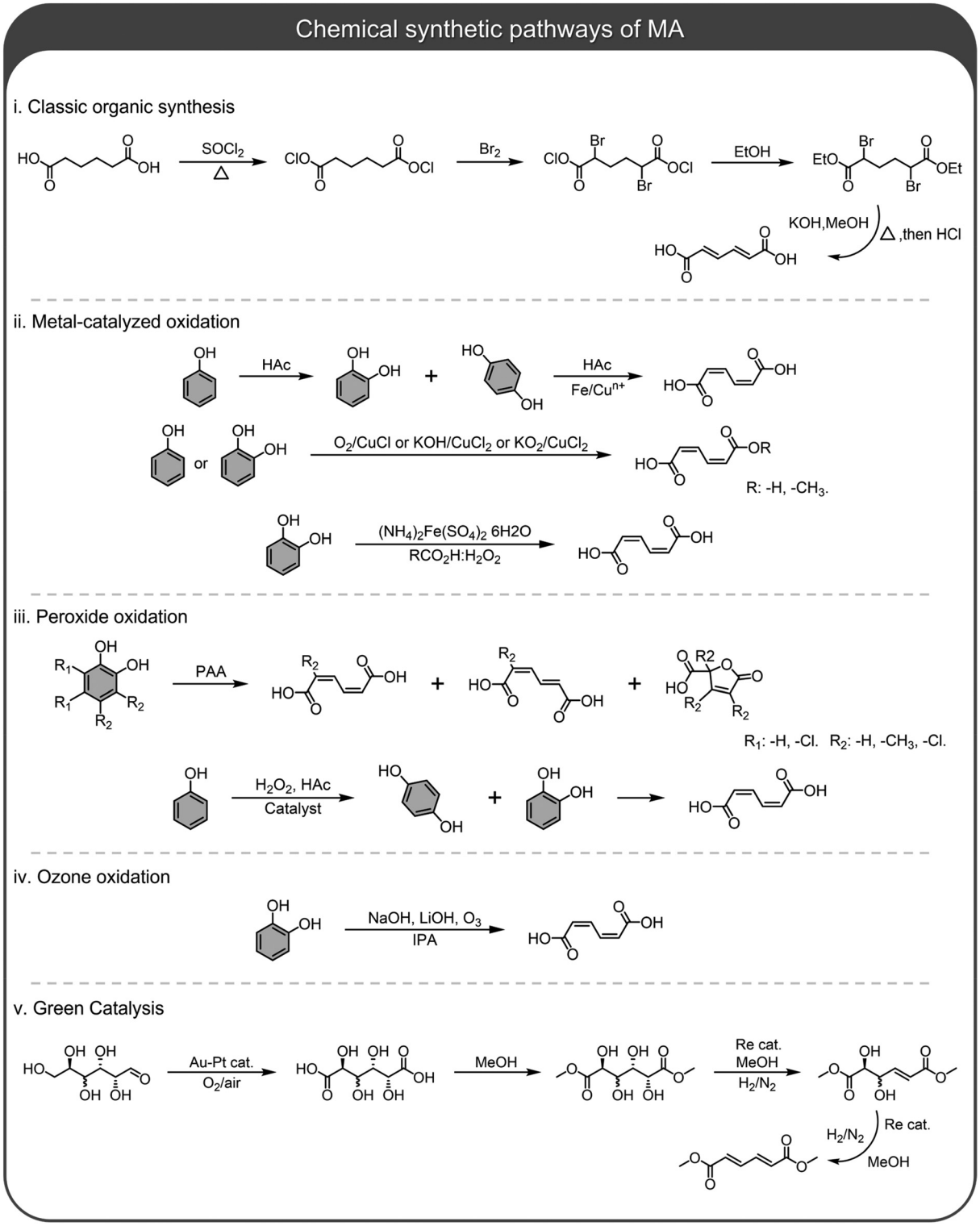

Fig. 4 Representative chemical syntheses of MA across different eras.[85–92] (i) Classic organic synthesis. (ii) Metal-catalyzed oxidation. Reprinted with permission from Pandell, *J. Org. Chem.*, 1976, **41**, 3992–3996. Copyright © 1976, American Chemical Society. Tsuji *et al.*, *Tetrahedron*, 1978, **34**, 641–644. Copyright © 1978 Published by Elsevier Ltd. (iii) Peroxide oxidation. Reprinted with permission from Rocha *et al.*, *J. Mol. Catal. Chem.*, 2002, **187**, 95–104. Copyright © 2002 Elsevier Science. Coupé *et al.*, *Green Chem.*, 2020, **22**, 6204–6211. Copyright © 2013 The Royal Society of Chemistry. (iv) Ozone oxidation. Reprinted with permission from Katayama *et al.*, *Molecules*, 2025, **30**, 201. Licensed under CC BY 4.0. (v) Green catalysis. Reprinted with permission from Hočevar *et al.*, *Angew. Chem. Int. Ed.*, 2020, **60**, 1244–1253. Copyright © 2020 Wiley-VCH GmbH.

(peracetic acid, performic acid, *etc.*), ozone (O_3), and molecular oxygen (O_2). Catalysts, predominantly metal-based (iron salts, copper salts, Fe complexes, metal phosphates, diselenide compounds), are required, with some reactions needing ligands (*e.g.*, tris(2-pyridylmethyl)amine) or solvent assistance (*e.g.*, pyridine, dichloromethane, methanol, formic acid). From a green chemistry perspective, most chemical conversion methods have significant drawbacks, such as multi-step reactions, use of toxic/hard-to-handle solvents (pyridine, dichloromethane), difficult separation and recovery of catalysts (homogeneous catalysts), and environmental toxicity and safety hazards. The combination of difficult-to-obtain feedstocks, harsh reaction conditions, and complex downstream processing hinders large-scale industrial production.

As early as 1946, Guha *et al.* first reported a two-step synthesis: reaction of adipic acid with thionyl chloride to form diethyl α,δ-dibromoadipate, followed by reaction with potassium hydroxide, methanol, and concentrated hydrochloric acid to produce MA, noting the existence of three stereoisomers.[85] In 1976, Pandell *et al.* introduced metal catalysts, developing a "biomimetic oxidation" pathway using phenol or catechol as feedstocks. Phenol is first hydroxylated to catechol and hydroquinone (rate-determining step, metal-independent); catechol, as a key intermediate, forms a metal–catechol complex with Fe/Cu, which is then rapidly oxidized to ccMA, albeit with a maximum yield of only 40%.[86] Tsuji and Takayanagi altered the reaction system and product type, using catechol/phenol in pyridine–alcohol mixed solvents with different oxidation systems (O_2/CuCl, KOH/$CuCl_2$, KO_2/$CuCl_2$) to synthesize ccMA monoesters, addressing the issue of catechol polymerization.[87] McKague *et al.* used various substituted catechols (containing alkyl, chloro, and dimeric groups) as feedstocks, synthesizing a series of substituted MAs *via* peracetic acid oxidation, expanding product structural diversity and enabling the preparation of multi-substituted and polymeric MAs.[88] In 2002, Rocha *et al.* introduced metal(IV) phosphates (*e.g.*, zirconium phosphate, tin phosphate, titanium phosphate) as catalysts for the selective synthesis of MA from phenol in an H_2O_2-acetic acid system, developing a novel catalytic system beyond traditional metal salts.[89,93] Van Ornum *et al.* first demonstrated the high efficiency of ozonolysis for oxidative cleavage of double bonds in a pharmaceutical synthesis context, providing process references for the oxidative cleavage of MA precursors (*e.g.*, catechol, alkylphenols).[94] Kooti and Jorfi developed a green NiO_2/CH_3COOH oxidation system, verifying its efficient oxidation capability for substrates like aromatic alcohols, thiophenols, and amines, offering catalyst design insights for the phenol to quinone to MA oxidation step in MA synthesis.[95] Giurg *et al.* achieved the regioselective synthesis of 2- and 3-substituted muconolactones from alkylphenols, providing a new feedstock route (alkylphenols) and catalytic system (diselenide/H_2O_2) for MA (obtainable *via* lactone hydrolysis).[81]

Subsequently, researchers have delved into green chemical synthesis routes for MA. Brigita Hočevar *et al.* developed a Re-based heterogeneous catalytic system under hydrogen-free conditions, using renewable galactaric acid as feedstock, carbon-supported Re catalyst (Re/C, activity enhanced after pretreatment), with Pd/C as a co-catalyst to promote the hydrogenation step; methanol served as the solvent, enabling *in situ* esterification to protect carboxyl groups from lactonization. At 120 °C under 0.5 MPa, N_2 atmosphere, muconate was hydrogenated to dimethyl adipate (yield 60.5%), with total dehydroxylation products (including muconate) yield reaching 63.6%; methanol acted as an endogenous hydrogen source, eliminating the need for external H_2 and avoiding corrosive reagents.[91] Coupé *et al.* developed an α-ZrP supported Cu(II) heterogeneous catalyst. At 30 °C, using formic acid/hydrogen peroxide (molar ratio 5 : 1) to generate performic acid *in situ*, phenol conversion reached 66% with ccMA selectivity of 60% (yield 40%). In a scaled-up experiment with 10 g phenol, ccMA yield was 39%, and the catalyst maintained 50% selectivity after 5 cycles, achieving one-step synthesis of phenol to catechol to MA, simplifying the reaction process and enhancing industrial potential.[90] Kohtaro Katayama *et al.* addressed the low yield issue in traditional ozone-based synthesis of MA by developing an ozone oxidation system in the presence of base. Adding three molar equivalents of NaOH allowed the generated ccMA to precipitate as a sodium salt and be removed from the reaction system, preventing its decomposition by excess ozone into byproducts such as glyoxalic acid and oxalic acid. Using isopropanol as the solvent and conducting the reaction at −40 °C, achieving a 56% ccMA yield in a single step. This method eliminates toxic reagents, simplifies operation, and significantly improves yield compared to conventional ozone synthesis, aligning with industrial green production requirements.[92]

2.2.2 Biological fermentation. Given the numerous drawbacks of chemical conversion methods, biological fermentation has emerged as a research hotspot in recent years. It primarily utilizes three types of renewable resources: glucose, lignin and its derivatives (*e.g.*, vanillin, *p*-coumaric acid, and other aromatic compounds), and other waste streams (*e.g.*, hydrolysis products of polyethylene terephthalate (PET), methane, industrial wastewater). Commonly used microorganisms include *Escherichia coli* (*E. coli*), *Corynebacterium glutamicum* (*C. glutamicum*), *Pseudomonas putida* (*P. putida*), and *Saccharomyces cerevisiae*.

Glucose is currently one of the most widely used feedstocks for MA biosynthesis because it is the preferred carbon source for most microorganisms (*e.g.*, *E. coli*, *C. glutamicum*, yeast), eliminating the need for complex carbon utilization pathway engineering. For instance, industrial strains like *E. coli*[96] and *C. glutamicum*[97,98] naturally possess efficient glucose transport systems (*e.g.*, PTS system) and metabolic enzymes, reducing the difficulty of strain modification. Furthermore, glucose can be extracted at low cost from renewable biomass like starch, sucrose, and cellulose (*e.g.*, corn, sugarcane, straw), with a mature global supply chain and stable prices.[99] Among these, obtaining glucose from lignocellulosic biomass (such as straw) requires effective pretreatment to overcome its inherent resistance to degradation, thereby releasing fermentable sugars.[100] Microorganisms can rapidly convert glucose into central metabolic intermediates – phosphoenolpyruvate (PEP) and ery-

throse-4-phosphate (E4P) – *via* glycolysis and the pentose phosphate pathway (PPP). These two compounds are direct precursors for 3-dehydroshikimate (DHS), a key intermediate in the MA synthesis pathway (*via* the shikimate pathway).[101–103]

The core pathway for MA synthesis from glucose (shikimate pathway branch) has been deeply elucidated and is readily tunable, currently yielding the highest titers. Key pathway: glucose → PEP/E4P → 3-deoxy-D-arabino-heptulosonic acid 7-phosphate (DAHP) → DHS → protocatechuic acid (PCA) → catechol (CAT) → ccMA (Fig. 5).[105–111] By knocking out genes of competing pathways (*e.g.*, *tyrR*, *ptsG* for aromatic amino acid synthesis), overexpressing key enzymes (*e.g.*, DHS dehydratase *aroZ*, PCA decarboxylase *aroY*, catechol 1,2-dioxygenase *catA*),[112,113] and relieving feedback inhibition (*e.g.*, using feed-

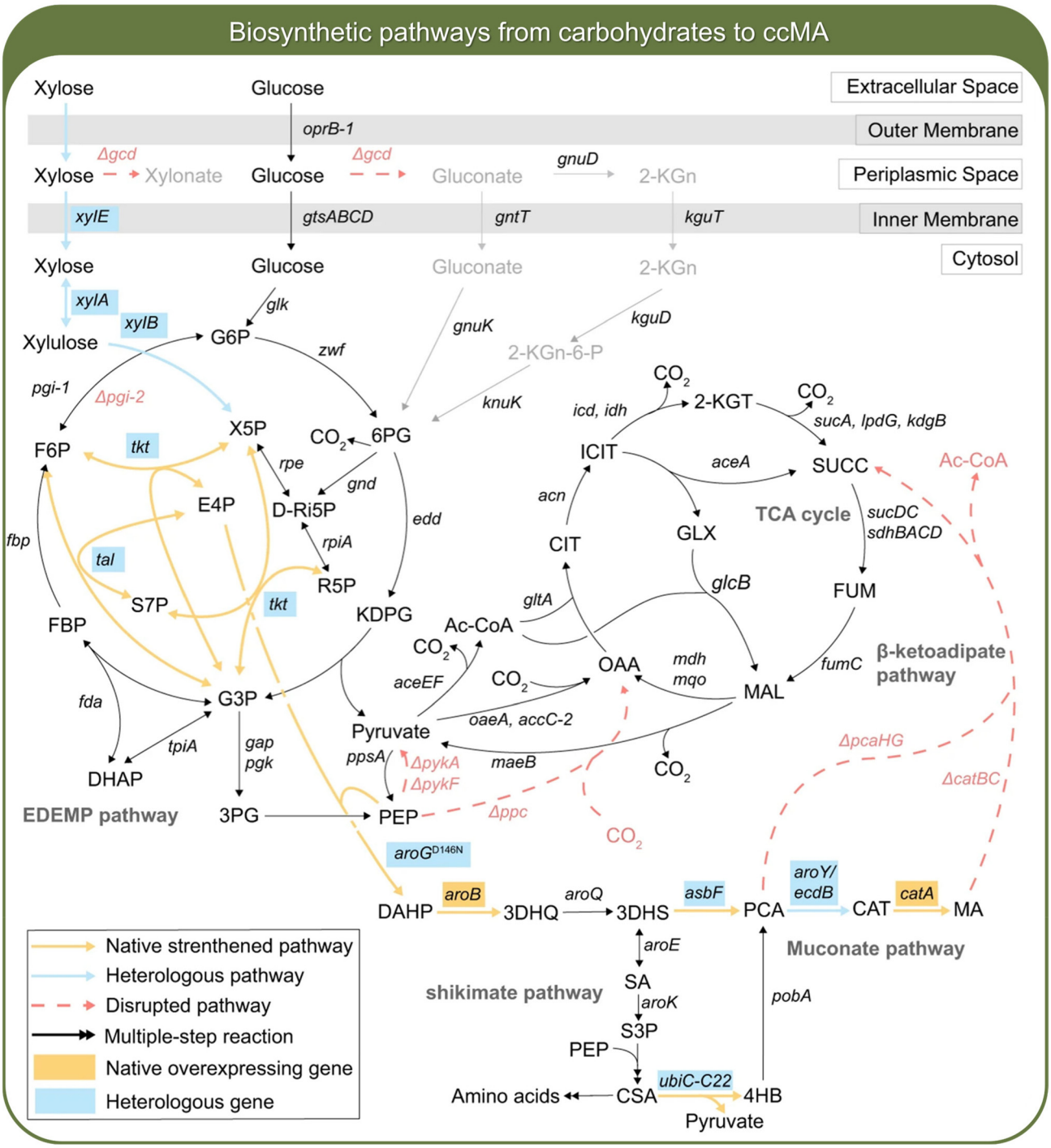

Fig. 5 Biosynthetic pathways used to produce MA from carbohydrates.[104] Adapted from Ling *et al.*, *Nat. Commun.* 2022, **13**, 4925, licensed under CC BY 4.0.

back-resistant DAHP synthase *aroG*^FBR), carbon flux diversion towards MA can be significantly enhanced. *Corynebacterium glutamicum* utilizing glucose achieved a ccMA titer of 88.2 g L^{-1} (5-L fed-batch fermentation),[98] and *Escherichia coli* reached 64.5 g L^{-1},[114] representing the highest levels among all feedstocks.

Besides glucose, lignin is another major feedstock for MA biofermentation. Lignin is the second most abundant natural polymer on earth (total reservoir estimated ~300 billion tons)[115,116,152] and a major byproduct of agricultural waste (straw, bagasse) and biorefining (cellulosic ethanol production).[117–119] Its status as an "industrial waste" means it doesn't compete with food crops (like corn and sugarcane for glucose) and helps address environmental issues associated with waste accumulation, aligning with the circular economy concept of green synthesis. Lignin is composed of aromatic units like syringyl, guaiacyl, and *p*-hydroxyphenyl, which can be catalytically degraded into aromatic monomers[120,121] (guaiacol,[122] vanillin,[117] *p*-coumaric acid,[123,124] ferulic acid,[125] hydroquinone,[70] *etc.*) (Fig. 6). These monomers are just key

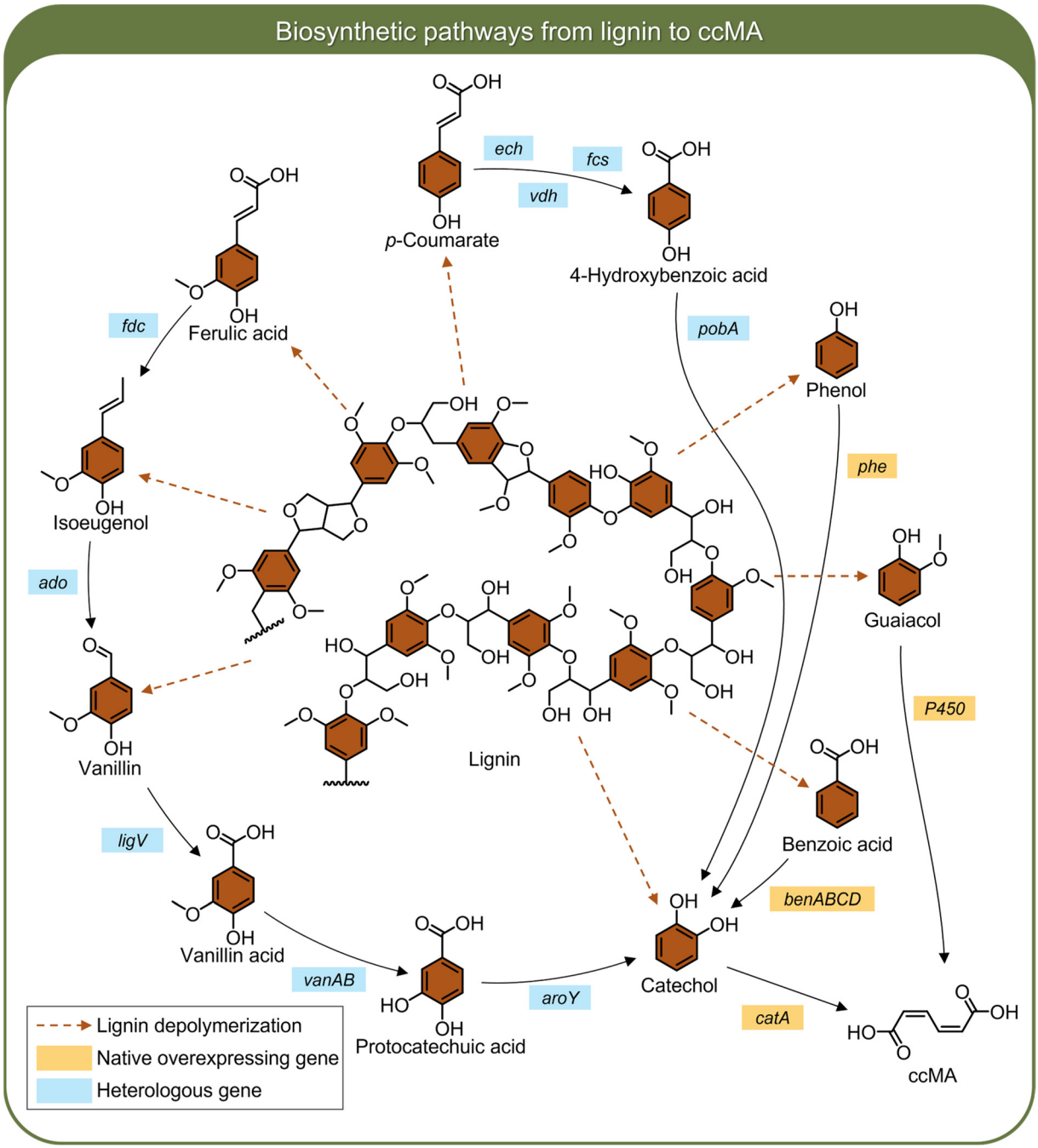

Fig. 6 Biosynthetic pathways used to produce MA from lignin.

precursors for MA synthesis – most aromatic monomers can be converted to catechol (CAT) *via* 1–3 enzymatic steps, and CAT requires only one enzymatic step (catalyzed by catechol 1,2-dioxygenase, *catA*) to generate ccMA with a theoretical molar yield of 100%.[126] The conversion of catechol → ccMA requires only *catA* catalysis. *C. glutamicum* strain using this substrate achieved a ccMA titer of 85 g L^{-1}.[97] *p*-Coumaric acid, *via* the 4-hydroxybenzoate (4HB) → protocatechuic acid (PCA) → CAT pathway, allowed *P. putida* KT2440-CJ242 to produce 49.7 g L^{-1} ccMA.[127]

Compared to glucose (a C6 sugar requiring reconstruction into aromatic precursors *via* the shikimate pathway) or xylose (metabolized *via* the Dahms pathway), lignin derivatives (C6 aromatic monomers) enter aromatic metabolic pathways directly without complex carbon chain rearrangement, offering higher carbon utilization efficiency. Strains like *Pseudomonas putida*,[70] *Corynebacterium glutamicum*,[106] and *Amycolatopsis* sp.[122] naturally possess the β-ketoadipate pathway (the core pathway for aromatic compound degradation) and can directly utilize lignin derivatives (*e.g.*, catechol, vanillic acid) to produce ccMA. Simple genetic modifications can block further MA metabolism, enabling product accumulation. However, phenolic and aldehyde compounds in lignin hydrolysates can be toxic to microbes.[70] Strategies like adaptive laboratory evolution (ALE), genome reduction (*e.g.*, *P. putida* EM42), or heterologous expression of tolerance genes can significantly enhance strain tolerance.[128,129] Direct use of unpurified lignin hydrolysates currently results in very low titers (~1.8 g L^{-1}), limiting industrial application.[97]

Additionally, other carbon sources like xylose, PET, glycerol, and methane can also be converted to MA[130–133] (Fig. 5 and 7). Xylose, a major component of hemicellulose found abundantly in agricultural waste (corn stover, bagasse) and forestry residues (sawdust), is a non-food biomass.[134] A key feature is its co-utilization with glucose (from cellulose),[135–137] addressing the carbon catabolite repression (CCR) issue in biomass hydrolysates – by modifying carbon catabolite repression genes, simultaneous consumption of both sugars can be achieved, enhancing overall biomass carbon utilization.[104,138] *P. putida* KT2440, through *xylA*/*xylB* overexpression + PPP gene (*tal*, *tkt*) optimization + ALE, produced 33.7 g L^{-1} ccMA from xylose (500 mL fed-batch fermentation).[104]

Polyethylene terephthalate (PET), one of the most common plastics, causes environmental pollution and resource waste after disposal. Existing PET recycling technologies (physical/chemical methods) face issues like low efficiency, high cost, or complex processes. Liu *et al.* metabolically engineered *P. putida* to secrete PET hydrolase extracellularly, degrading PET to Terephthalic acid (TPA), which was then converted to PCA *via* the *tph* gene cluster for entry into the MA synthesis pathway. This approach needs to resolve the temperature discrepancy between leaf-branch compost cutinase hydrolysis and strain growth.[130] Subsequently, Kim *et al.* used microwave-assisted hydrolysis to depolymerize PET into TPA, followed by its precipitation and separation. Using *E. coli* as the chassis and the same pathway, they achieved an MA yield of 85.4%. Further optimization is needed for methyl donor supply in vanillic acid synthesis and byproduct (catechol) accumulation in pyrogallol synthesis.[131]

Methane (CH_4) is the second most important greenhouse gas and also a low-cost, non-food carbon source. Henard *et al.* engineered methanotrophic bacteria to express three key enzymes *via* an inducible tetracycline (*tet*) promoter, utilizing the shikimate pathway intermediate (dehydroshikimate, DHS) to synthesize MA, achieving a yield of 2.8 ± 0.04 mg MA per g CH_4. This pioneering work demonstrated the first biological conversion of methane to MA, offering a new route for valorizing greenhouse gas (methane) and green MA production. However, two major challenges need addressing: first, the shikimate metabolic network in methanotrophs is not fully elucidated, requiring further genomic functional exploration; second, optimizing gas mass transfer efficiency and balancing strain growth with production rate necessitate future fermentation process and strain engineering improvements.[132]

Glycerol, a byproduct of biodiesel production, is a cheap, renewable carbon source, and its conversion into high-value chemicals holds significant scientific and commercial value. Traditional MA synthesis pathways from glycerol (*e.g.*, *via* DHS or anthranilic acid) suffer from requirements for expensive precursors and low efficiency of rate-limiting steps. Lin *et al.* engineered a phenylalanine-overproducing *E. coli* ATCC31884, constructing and optimizing a pathway in three steps: building a high-shikimate producing strain, converting shikimate to salicylic acid, and converting salicylic acid to MA. The modularly optimized strain (LS-8) achieved an MA titer of 1.5 g L^{-1} in shake flasks within 48 h.[139] Zhang *et al.* addressed issues in traditional single-strain MA production, such as high metabolic burden, intermediate accumulation (*e.g.*, DHS), and low yield, by designing a two-strain co-culture system with division of labor: an upstream strain producing DHS and a downstream strain converting DHS to MA.[133] Wang *et al.* identified that traditional microbial MA production often relies on plasmids and inducers, leading to high metabolic burden and genetic instability. They chromosomally integrated the endogenous ubiquinone synthesis pathway with the PCA degradation pathway in *Pseudomonas chlororaphis* HT66, eliminating plasmid dependency.[140]

3. Polymerization strategies for muconic acid

The presence of both dicarboxylic acid functional groups and conjugated double bonds in MA provides its potential for polymer formation. Current research on MA-based polymers primarily focuses on three directions: i. utilizing the dicarboxylic acid groups for polycondensation with various diols or diamines to form unsaturated polyesters, polyamides, *etc.*, ii. utilizing the conjugated double bonds for addition polymerization to form structures similar to polybutadiene, or for copolymerization with other vinyl monomers. iii. utilizing carboxyl groups to coordinate with various metal ions and nitrogen-containing ligands, forming coordination polymers (Fig. 8 and 9).

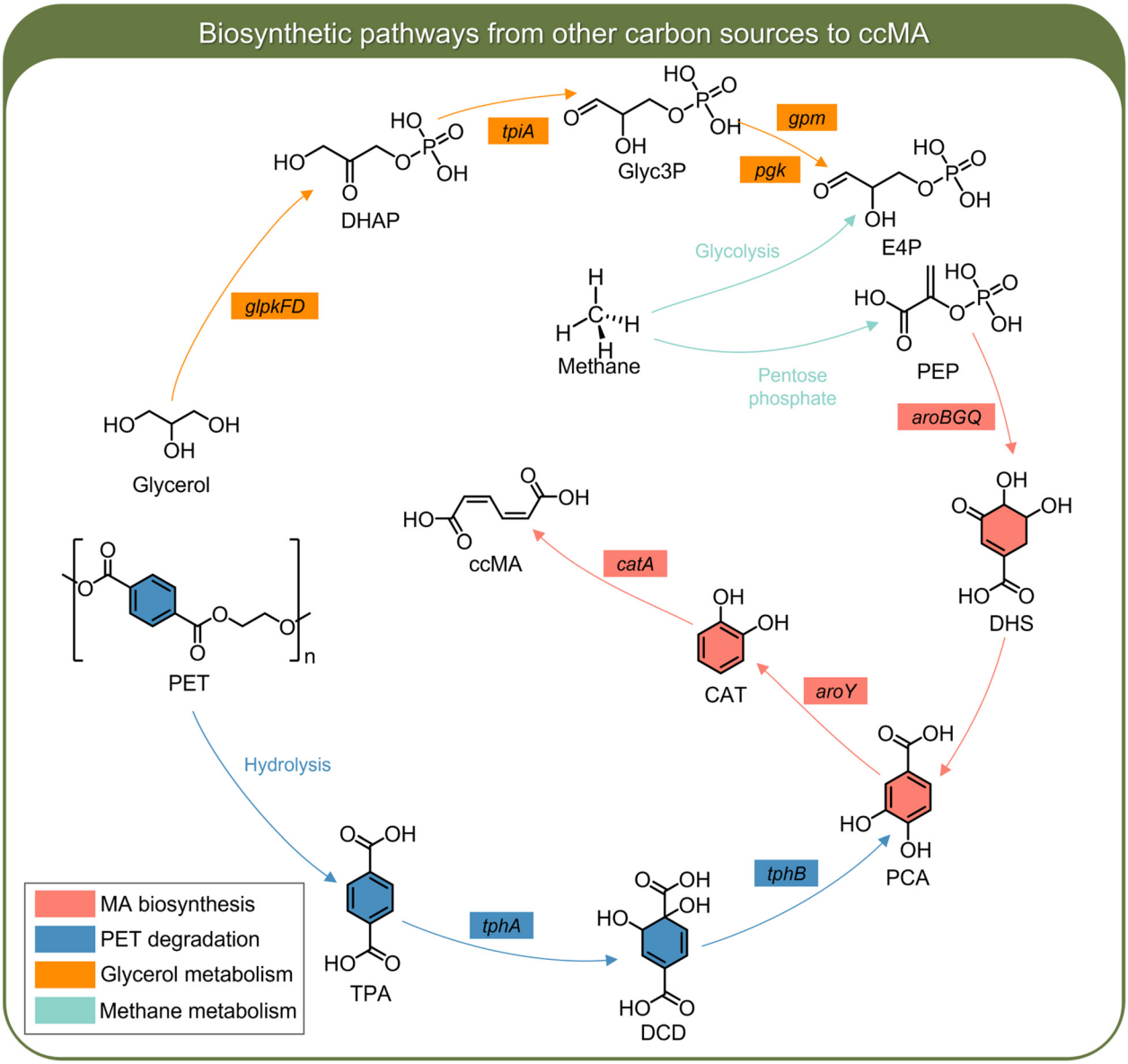

Fig. 7 Biosynthetic pathways used to produce MA from other carbon sources.

3.1 Polycondensation

The key feature of polycondensation *via* the dicarboxylic acid groups of MA is the retention of the conjugated double bonds within the polymer backbone. This preserves the potential for post-polymerization modification, such as crosslinking with reactive diluents or introducing other functional groups to alter polymer properties and expand functionality.[142]

Rorrer *et al.* were among the first to directly use ccMA for the synthesis of unsaturated polyesters (UPEs), copolymerizing it with succinic acid and various aliphatic diols (ethylene glycol, propylene glycol, 1,4-butanediol, 1,6-hexanediol). They compared differences between using dimethyl *cis*,*cis*-muconate and ccMA directly. The low molecular weight copolymers were compounded with styrene and impregnated into glass fibers to prepare composites. MA incorporation increased the glass transition temperature (T_g, indicating enhanced rigidity) of the UPEs but decreased the melting temperature (T_m) and degradation temperature. Dimethyl muconate copolymerization achieved stoichiometric incorporation, forming random copolymers, whereas direct MA copolymerization resulted in "gradient copolymers" (exhibiting two T_gs). PBS-MA/styrene glass fiber composites showed shear modulus exceeding 30 GPa (comparable to commercial FRP), T_g up to 90 °C, and good thermal stability (degradation temperature ~400 °C). By varying MA loading and copolymerization method (acid/ester), the molecular structure of the UPE (gradient/random) could be tuned, thereby customizing composite properties.[20] Subsequently, they expanded the substrate to ttMA and replaced styrene with methacrylic acid or a mixture of

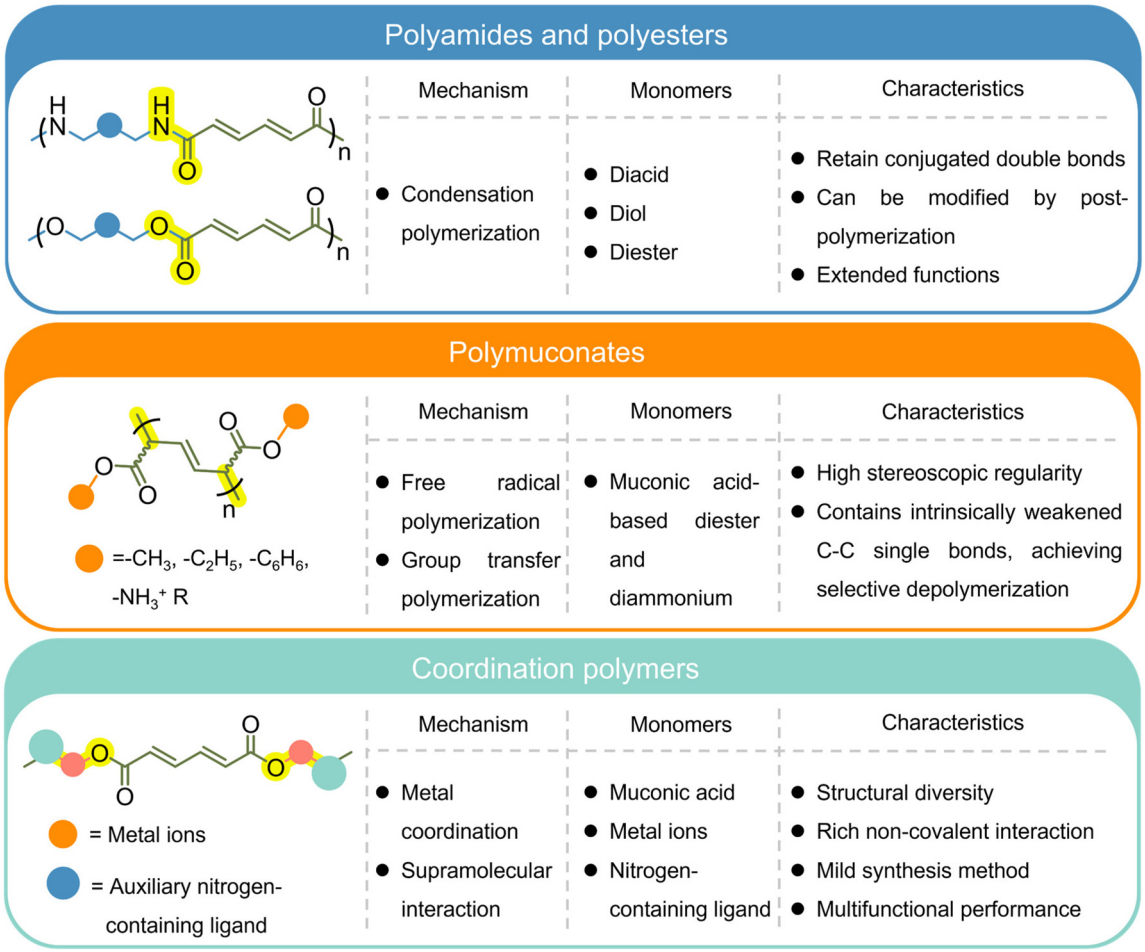

Fig. 8 Three types of MA-based polymers and their polymerization mechanisms, monomers, and key characteristics.

methacrylic acid and cinnamic acid as reactive diluents, creating a fully bio-based unsaturated polyester system for FRP. This was compared with traditional petroleum-based UPE systems using maleic anhydride, fumaric acid, and styrene. Results showed that at equivalent olefin monomer loading, FRPs based on ttMA exhibited the highest shear modulus, storage modulus, and T_g, and the lowest loss modulus. When using methacrylic acid–cinnamic acid mixture as the diluent, FRP performance matched that of the styrene system while avoiding styrene's toxicity. Furthermore, ttMA, with only 1/3 the monomer loading (number of double bonds only 2/3 that of maleic anhydride), achieved storage modulus and T_g comparable to maleic anhydride-based systems, with superior loss modulus performance. This demonstrates that MA can directly serve as a renewable UPE monomer, its glass fiber composites meeting performance standards, offering a green alternative path for commercial unsaturated polyesters while expanding the functional application scenarios for biomass-based monomers.[18]

Existing UPE synthesis often suffers from double bond isomerization/saturation, making it difficult to obtain high molecular weight products. Yu *et al.* addressed this by using fully bio-based HA and fumaric acid (FA) as monomers, with stannous octoate as a catalyst and 4-methoxyphenol as a radical inhibitor, performing melt polycondensation with 1,4-butanediol to prepare high molecular weight unsaturated copolyesters (PBHBF). While the conjugated double bonds in MA enhance molecular thermodynamic stability, they also increase the chemical reactivity of the double bonds. In HA, the double bond and carboxyl group are separated by two methylene groups, forming an isolated double bond (no conjugation). This structure results in a uniform electron cloud distribution around the double bond: it lacks high electron density and does not suffer from excessive electron delocalization due to conjugation, making it one of the most "chemically inert" double bond structures in polymerization. PBHBF exhibited tensile strength (29.6–42.6 MPa) and elongation at break (180%–847%) superior to linear low-density polyethylene (LLDPE) and most saturated aliphatic polyesters (*e.g.*, PBS, PBAT). PBH4BF60, in particular, showed an elongation at break of 847%, combining rigidity and toughness.[19] Naves *et al.* copolymerized renewable sugar-derived isosorbide and isomannide (known for high rigidity and thermal stability) with diethyl adipate and diethyl *trans*-β-hydromuconate, using

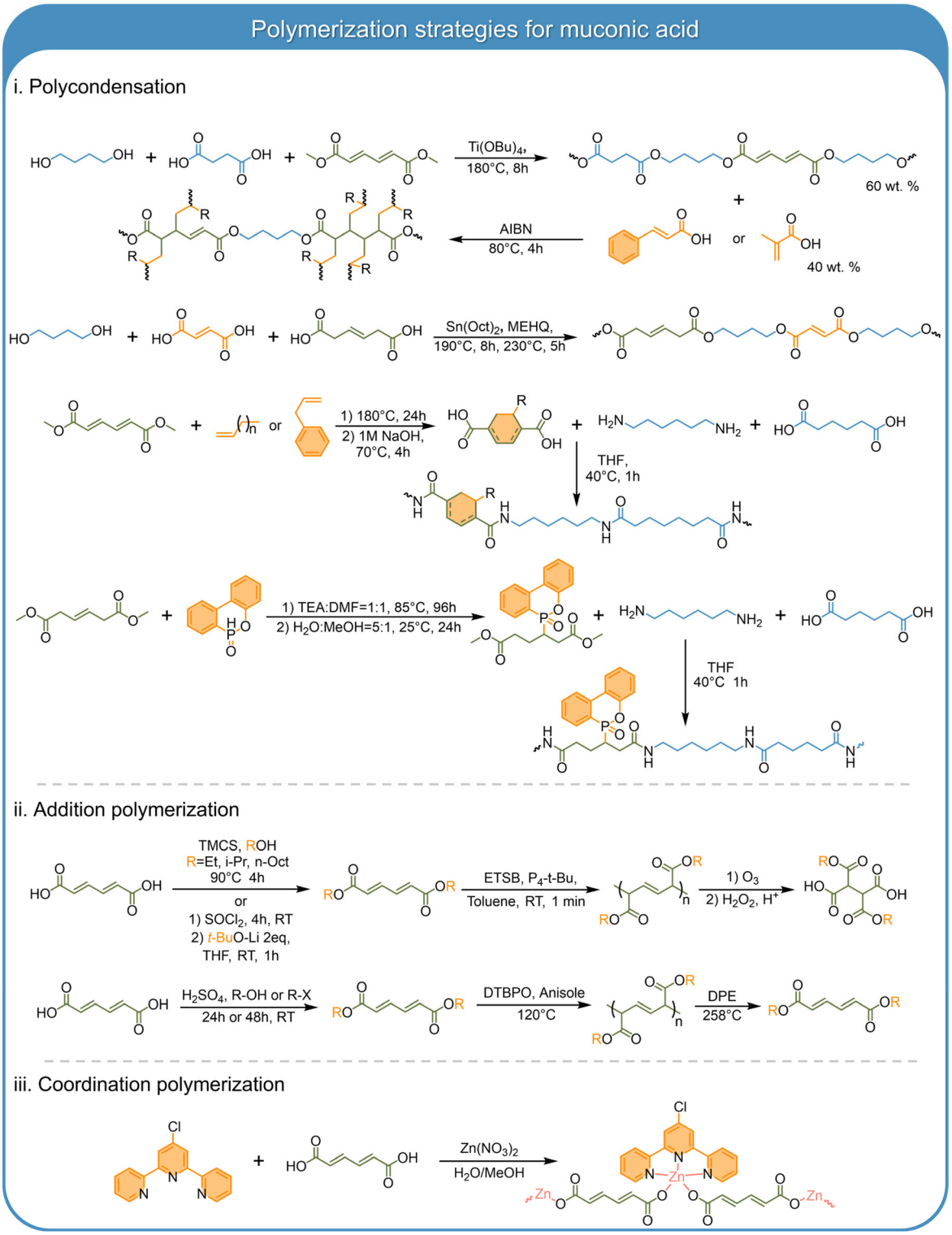

Fig. 9 Synthesis processes of different MA-based polymers.[18,19,22,23,25,30,141] (i) Polycondensation. Reprinted with permission from Rorrer *et al.*, *Green Chem.*, 2017, **19**, 2812–2825. Copyright © 2017 The Royal Society of Chemistry. Yu *et al.*, *ACS Sustain. Chem. Eng.*, 2019, **7**, 6859–6869. Copyright © 2019 American Chemical Society. Carter *et al.*, *RSC Sustain.*, 2024, **2**, 2968–2978. Copyright © 2024 The Royal Society of Chemistry. Carter *et al.*, *J. Am. Chem. Soc.*, 2022, **144**, 9548–9553. Copyright © 2022 American Chemical Society. (ii) Addition polymerization. Reprinted with permission from Dardé *et al.*, *Angew. Chem. Int. Ed.*, 2024, **63**, e202411249. Copyright © 2024 Wiley-VCH GmbH. Hu *et al.*, *Nat. Chem. Eng.*, 2025, **2**, 130–141. Copyright © 2025, under exclusive licence to Springer Nature America, Inc. (iii) Coordination polymerization. Reprinted with permission from Bhunia *et al.*, *New J. Chem.*, 2021, **45**, 13941–13948. Copyright © 2021 The Royal Society of Chemistry.

CALB as catalyst and azeotropic removal of ethanol in cyclohexane-toluene mixed solvent.[143]

Besides using more stable MA monomers, Maniar *et al.* employed enzyme-catalyzed polymerization (immobilized *Candida Antarctica* Lipase B, CALB) to develop a green, mild synthesis route for MA-based unsaturated polyesters. This approach avoids double-bond side reactions caused by traditional metal catalysts and harsh conditions, offering a greener alternative. They copolymerized dimethyl esters of the three MA isomers and dimethyl *trans*-β-hydromuconate with aliphatic diols of varying chain lengths (1,4-butanediol to 1,12-dodecanediol). Results indicated enzymatic selectivity: CALB showed higher catalytic activity towards the more open-structured *cis*,*trans*-muconate ester compared to the closed-structure *cis*,*cis*-isomer. Polymers based on ctMUC reached molecular weights up to 21 200 g mol^{-1}, while those based on ccMUC only reached 2210–2900 g mol^{-1}. ttMUC, due to its rigid double bonds and high steric hindrance, yielded low molecular weight polymers (max 3100 g mol^{-1}). TBHM, with its flexible isolated double bond, achieved high molecular weights (up to 21 900 g mol^{-1}). They also explored competitive copolymerization between saturated (dimethyl adipate) and unsaturated monomers, finding CALB had higher affinity for TBHM with its isolated double bond. In copolymerization, the saturated monomer polymerizes preferentially, requiring adjustment of monomer ratios to balance molecular weight.[144,145]

The conjugated double bonds in MA grant it potential for Diels–Alder (DA) cycloaddition reactions. Prerana Carter *et al.* utilized ttMA or its dimethyl ester (dmttM) as starting materials, reacting them with different dienophiles (ethylene, 1-octene, 1-tetradecene, allylbenzene) *via* DA reaction to synthesize a series of cyclic diacid monomers. These monomers incorporated long alkyl chains (enhancing hydrophobicity) or aromatic groups (improving flame retardancy). These diacids were then copolymerized with hexamethylenediamine and adipic acid to prepare performance-enhanced nylon 66 copolymers, enabling performance customization on demand rather than simple replacement. The copolymers had slightly lower molecular weights and melting points compared to pure nylon 66. Although crystallinity decreased, it did not significantly impair mechanical properties, and the storage modulus was even higher than that of pure nylon 66. Copolymers containing long alkyl chains showed 40%–70% reduction in water absorption compared to pure nylon 66, with contact angle increasing from 75° to 87°, while retaining the crystal structure and glass transition temperature of nylon 66. Copolymers containing aromatic groups exhibited a char yield of 6.1% at 500 °C, doubling that of pure nylon 66 (2.9%), and the thermal degradation temperature increased by 7 °C.[23] Also addressing the flammability of nylon 66, Carter *et al.* noted that traditional additive flame retardants (*e.g.*, DOPO) can improve flame resistance but often lead to reduced mechanical properties and potential leaching over time. They therefore used the MA derivative *trans*-3-hexenedioic acid (t3HDA) as a starting material, covalently grafting the flame retardant DOPO onto the monomer molecule *via* phospha-Michael addition, and then copolymerizing it with nylon 66 to create "intrinsically flame-retardant" copolymers, overcoming the drawbacks of additive flame retardants. Dimethyl t3HDA was isomerized under basic catalysis to generate the more reactive dimethyl *trans*-2-hexenedioate (dmt2HD), which then underwent phospha-Michael addition with 9,10-dihydro-9-oxa-10-phosphaphenanthrene-10-oxide (DOPO) to graft DOPO. They compared two methods of DOPO incorporation: physical blending (PA66-5B/10B, DOPO content 5/10 wt%) and covalent copolymerization (PA66-5F/10F, DOPO content 5/10 wt%). PA66-10F showed a lower fire growth capacity (FGC) of 302.6 J g^{-1} K^{-1} compared to PA66-10B (327.5 J g^{-1} K^{-1}), with a more significant reduction in total heat release (THR). PA66-5F exhibited higher tensile strength than both pure nylon 66 and PA66-5B. Processing difficulties (T_m close to degradation temperature) made PA66-10F relatively brittle, but its T_g was significantly higher than that of PA66-10B.[22]

3.2 Addition polymerization

Polymerization *via* the double bonds involves prior esterification or amination of MA, followed by free radical polymerization. However, direct free radical polymerization of MA derivatives typically yields atactic polymers. Therefore, topochemical polymerization and organocatalytic group transfer polymerization have been extensively studied to obtain stereoregular polymuconates (or ammonium salts). Primary polymerization methods include: (1) Solid-state (topochemical) polymerization: relies on ordered molecular packing (*e.g.*, columnar arrangement) in monomer crystals, achieving polymerization through minimal molecular motion, yielding products with high stereoregularity. (2) Bulk polymerization: initiated in the molten state (solvent-free), suitable for some muconate esters. (3) Solution polymerization: conducted in solvent (*e.g.*, anisole). Initiation systems primarily include: photopolymerization (UV light, sunlight, scattered light), radiation polymerization (γ-radiation, X-ray radiation), and initiators (*e.g.*, DTBPO).

In 1977, Bando *et al.* first performed free radical polymerization on MA and its derivatives. Since MA has poor solubility in most organic solvents, only slightly dissolving in DMSO and pyridine, they used DMSO as solvent and azobisisobutyronitrile (AIBN) as initiator, achieving yields of 6%–36%. Polymerization of ethyl muconate (EMU) in benzene solvent yielded 9.7%; using an anionic catalyst (*n*-butyllithium) increased the yield to 34.5%, while cationic catalysts showed no activity. They also studied copolymerization behavior with styrene and acrylonitrile.[26] Later, in 1996, Matsumoto *et al.* synthesized dialkyl muconates of the three configurations (cc, ct, tt). When using di-*tert*-butyl peroxide as initiator for bulk polymerization at 120 °C, all monomers (regardless of configuration) generated high molecular weight polymers (number-average molecular weight, M_n = (1–4) × 10^5 g mol^{-1}) with yields of 25%–79% over 3–4 hours. The cyclohexyl ester, benefiting from the large steric hindrance of the ester group and high system viscosity which suppressed chain termination

reactions, gave the highest yield (78.9%) and molecular weight (M_n = 4.09 × 10^5 g mol^{-1}). Solution polymerization (*e.g.*, in *p*-xylene or DMF), due to low monomer concentration and solvent chain transfer, only produced low molecular weight polymers (M_n = (0.7–1.5) × 10^4 g mol^{-1}).[24] In 2019, Quintens *et al.* synthesized a series of *trans*,*trans*-dialkyl muconates to enhance monomer and polymer solubility, avoiding interference with polymerization kinetics. By optimizing temperature (120 °C), initiator (di-*tert*-butyl peroxide, DTBPO), solvent (anisole, green and recyclable), and monomer concentration (2 mol L^{-1}), they achieved efficient polymerization of dialkyl muconates, obtaining polymers with molecular weights exceeding 10^4 g mol^{-1}. The polymerization was relatively slow (48 hours), and high monomer purity was crucial for forming high molecular weight products, requiring additional purification steps like liquid–liquid extraction and basic alumina filtration. They also pioneered the use of RAFT for controlled polymerization of muconates, using a conventional trithiocarbonate (CPD-TTC) as the regulating agent, achieving precise molecular weight control in the range of 2–20 × 10^3 g mol^{-1} with low dispersity ($Đ$ = 1.2–1.4), laying the groundwork for developing high-value-added materials.[27]

Muconate esters in the crystalline state can undergo topochemical polymerization upon light irradiation. Matsumoto *et al.* discovered in 1996 that diethyl (*Z*,*Z*)-muconate crystals undergo topochemical polymerization upon UV irradiation, generating ultra-high molecular weight, highly stereoregular triactic polymers (*trans*-1,4-meso-disyndiotactic or isotactic structure). The crystals bent during polymerization and formed fibrous structures; other isomers (*e.g.*, (*E*,*E*)-, (*E*,*Z*)-) lacked this reactivity. They later expanded the substrate to dibenzylammonium (*Z*,*Z*)-muconate, which polymerized under UV or sunlight, yielding crystalline polymers insoluble in water, organic solvents, and acids/bases. These could be hydrolyzed with HCl to poly(muconic acid) (PMA), which could then be reacted with amines to regenerate ammonium salt polymers. The photoreactivity of dibenzylammonium (*Z*,*Z*)-muconate is controlled by the crystal lattice: columnar stacking leads to topochemical polymerization, while layered structures cause isomerization. The 2D hydrogen-bonding network formed between primary ammonium cations and carboxylate anions is key to constructing different stacking structures.[24] Relying on photoinitiation (UV) faces issues like uneven irradiation (surface reaction) and potential need for photosensitizers. γ-Rays, with their strong penetrating power, enable uniform initiation within the crystal. Polymerization yield is affected by crystal size, temperature, and radiation dose, with high doses causing polymer degradation.[43] In 2000, Odani and Matsumoto explored the possibility of topochemical polymerization for (*E*,*E*)-MA derivatives. The naphthyl group in the 1-naphthylmethylammonium salt formed a columnar structure *via* π-stacking interactions favorable for topochemical polymerization. They found that regardless of monomer configuration ((*Z*,*Z*) or (*E*,*E*)), as long as suitable molecular packing (*e.g.*, translational columnar stacking) is formed, topochemical polymerization can generate stereoregular polymers with a meso-diisotactic-*trans*-2,5 structure. Topochemical polymerization allows precise control over polymer tacticity and molecular weight. The resulting layered crystals of polymuconate derivatives exhibit efficient and reversible intercalation capability for alkylamines, with intercalation behavior tunable by amine structure and solvent polarity. Functional group modulation is possible *via* hydrolysis-intercalation reactions, enabling the design of functional organic solids (*e.g.*, for molecular recognition, separation materials).[37] Previous studies confirmed the importance of π-orbital overlap in muconate ester polymerization. Thus, tuning molecular stacking *via* weak interactions to optimize π-orbital overlap became a viable strategy. A halogen substitution strategy was introduced, utilizing halogen–halogen and CH/π weak interactions as supramolecular synthons in crystal engineering to control the molecular stacking structure of muconate derivatives.[35] Addressing the earlier reliance on light, X-ray, or γ-ray initiation, which involves operational complexity (radiation source), safety concerns, and high cost, they explored radiation-source-free topochemical polymerization of 4-chlorobenzyl (*Z*,*Z*)-muconate. To tackle issues associated with traditional synthesis using organic solvents (methanol, chloroform), such as environmental pollution, cost, and inability to intercalate poorly soluble amines, a solvent-free process was developed. Mechanical grinding achieved a four-step sequence: "monomer synthesis (yield 92%–94%) → polymerization (yield 76%–87% for dodecylammonium salt) → PMA conversion (250 °C vacuum pyrolysis for 2 h) → intercalation (91% conversion with *tert*-butylamine)".[49,50] However, precise control over polymer chain orientation remained challenging, limiting applications in high-performance materials (*e.g.*, oriented fibers, electronic devices). Utilizing the lattice matching of inorganic crystal substrates enables chain orientation control. Polarized UV light can selectively initiate polymerization of muconate ester crystals aligned in specific directions on KCl substrates, yielding polymer films with uniaxial orientation. The polymerized films exhibited a cross-grid structure, and polymer fibers could make right-angle turns at grain boundaries while maintaining crystalline continuity.[63]

Group transfer polymerization (GTP), a controlled polymerization method, has been widely applied to monomers like methacrylates. In 1988, W. R. Hertler studied the GTP of various unsaturated esters, including diethyl muconate, achieving high stereoselectivity for all-1,4-addition and lower dispersity, and proposed a mechanistic hypothesis.[146] Thomas Dardé *et al.* subsequently conducted more in-depth studies. Using *trans*,*trans*-diethyl muconate (DEM) as an example, they achieved 100% conversion within 1 minute, significantly faster than traditional RAFT polymerization. By adjusting the monomer/initiator ratio, polymer molecular weight (M_n) could be controlled, with dispersity ($Đ$) mostly between 1.30–1.72. They successfully demonstrated chain extension of homopolymers and synthesized all-muconate-based block copolymers. The reaction required no purification of intermediates and could be completed within 3 minutes. Changing the alkyl side chain structure significantly tuned the polymer's T_g. Various

post-polymerization modifications (PPM) were possible: hydrolysis of the ester groups yielded water-soluble PMA with the double bond structure intact; reaction of PD*t*BuM with *m*-chloroperoxybenzoic acid (*m*CPBA) converted the double bonds to epoxy groups, increasing T_g from 9.3 °C to 29.2 °C, significantly enhancing rigidity. Leveraging the C=C double bonds in the backbone, rapid degradation *via* ozonolysis was achieved, degrading high molecular weight polymers to low molecular weight oligomers within minutes, ultimately producing dicarboxylic acid diesters. These degradation products could serve as Gemini surfactants (with low critical micelle concentration) for preparing vesicle structures, with potential applications in pharmaceuticals and cosmetics, enabling "upcycling".[141]

To develop scalable, bio-sourced, and depolymerizable polydienes, the key lies in molecular design to intrinsically weaken carbon–carbon (C–C) bonds, enabling closed-loop recycling while balancing performance and economics.[28] Letian Dou *et al.* started from ttMA, synthesizing six muconate ester monomers with different ester substituents *via* esterification. They employed free radical polymerization using di-*tert*-butyl peroxide (DTBP) as initiator and anisole as solvent at 120 °C for 48 hours. Using ME-B and ME-Me as models, they prepared a series of copolymers (*e.g.*, PolyME-Me3B7) by varying monomer feed ratios. Gel permeation chromatography (GPC) data showed ME-B homopolymer had the highest molecular weight (M_w = 469 kDa, $Đ$ = 1.53). Copolymer molecular weight increased with ME-B content. ME-Et exhibited an elongation at break of 2170%, while ME-Cb and ME-2F showed only ~2% elongation (rigid). ME-B (462%) combined elasticity and strength. As ME-B content increased, copolymers transitioned from rigid (*e.g.*, PolyME-Me7B3, elongation at break 2.02%) to elastic (*e.g.*, PolyME-Me1B9, elongation at break 220%), matching the performance range of commercial polymers like PS and PET. PolyME-Me3B7 showed no significant changes in appearance, mass, or mechanical properties under harsh conditions, including acid, base, UV (350 nm), and heating at 60 °C. Upon heating to 258 °C, cleavage occurred at the intrinsically weakened C–C bonds. Monomer recovery rates for ME-Me, ME-Et, *etc.*, exceeded 65%, with byproducts mainly being Diels–Alder adducts (~20%), achieving a complete monomer to polymer to monomer cycle. NMR spectra of recovered monomers closely matched those of fresh monomers, and polymer performance showed no degradation after recycling.[25] Subsequently, they developed a solvent-free, catalyst-free polymerization strategy initiated by UV light (315–400 nm), achieving M_n up to 1210 kDa, dispersity of 1.5, and >99.5% 1,4-addition structure (compared to ~2% defects in traditional free radical polymerization). Concurrently, they demonstrated one-pot synthesis of ABA triblock copolymers (tensile strength 3.5 MPa, elongation at break 615%) and ABS-like plastics (T_g = 83 °C, tensile strength 52 MPa). Polymuconates depolymerized to monomers at 250 °C (recovery yield 80%–92%); the triblock copolymer yielded 86% monomer recovery, and the ABS-like material yielded 10% muconate, 42% styrene, and 75% acrylonitrile recovery. This work addresses issues in traditional polydiene synthesis (solvent/catalyst dependence, difficult recycling) and topochemical polymerization (structural regularity but difficulty in preparing complex architectures like block copolymers and poor processability).[84]

3.3 Coordination polymerization

The core advantage of MA for coordination polymerization lies in its combination of two carboxyl groups (–COOH) and a conjugated diene system (C=C–C=C), which synergistically meet the key requirements. The carboxyl groups, under basic conditions (*e.g.*, NaOH, triethylamine) or metal ion induction, readily deprotonate to form the divalent muconate dianion (muc^{2-}). Through the oxygen atoms of the carboxylate groups ($-O^-$), it forms stable coordination bonds with metal ions (Ag^+, Zn^{2+}, Cu^{2+}, Ni^{2+}, *etc.*), enabling monodentate/bidentate coordination modes: *e.g.*, bidentate chelation with Zn^{2+} (Zn–O bond length 1.93–1.96 Å) or monodentate bridging with Ag^+ (Ag–O bond length 2.66–2.80 Å). It can also act as a bridging ligand to extend dimensionality: by connecting adjacent metal ions through its two carboxylate groups, it can construct 1D chains (*e.g.*, Ni^{2+}-muc chain), 2D layers (*e.g.*, Cu^{2+}-muc square grid), or 3D networks (*e.g.*, Ag^+-muc sandwich structures with auxiliary ligands), serving as the core skeleton for building high-dimensional structures in coordination polymers. Although the conjugated double bonds do not directly participate in metal coordination, they can expand ligand diversity through *in situ* chemical reactions, indirectly enhancing coordination capability. For example, reaction with amines (ethylenediamine, piperazine) *via* double Michael addition generates new ligands containing heterocycles (*e.g.*, piperazine-2,3-diacetate), which contain both N and O coordination sites and can form more stable chelates with ions like Ni^{2+}. The conjugated system of the double bond can also form π–π stacking interactions with the aromatic rings of auxiliary ligands (such as bipyridine and benzimidazole), further stabilizing the 2D interlayer structure and preventing collapse of the higher-dimensional framework.

The molecular structure of MA combines a rigid conjugated backbone with rotatable carboxyl arms. This equilibrium enables adaptation to diverse metal ions and reaction conditions, facilitating the formation of various topological structures. The rigid conjugated backbone ensures linearity and geometric stability, preventing excessive distortion during coordination. For instance, when constructing a 2D square lattice, the conjugated backbone of vicinal conjugated acids functions as the edges. The flexible carboxyl arms allow the oxygen atom to adjust its coordination angle based on the metal ion's coordination number (*e.g.*, Ag^+'s 2-coordination, Zn^{2+}'s 4-coordination), accommodating different metal coordination geometries (*e.g.*, Zn^{2+}'s tetrahedral, Cu^{2+}'s octahedral).

Common methods for coordination polymerization include hydrothermal/solvothermal synthesis (105–160 °C), ultrasound-assisted methods (160 W, 40 kHz), or room-temperature layering techniques. MA/muconate is soluble in water or water-methanol mixtures, eliminating the need for toxic organic sol-

vents (*e.g.*, DMF, DMSO). The polarity of the carboxylate groups promotes uniform mixing with metal salts (*e.g.*, $AgNO_3$, $Zn(OAc)_2$), reducing phase separation and improving polymerization homogeneity. The process often requires no high temperature/pressure or special catalysts; coordination polymerization can be achieved simply by adjusting pH (*e.g.*, adding NaOH for deprotonation) and temperature. For example, using ultrasound for 15 minutes followed by room-temperature standing for 5 days achieved an 81% yield.

4. Applications of MA-based polymers

MA-based polymers demonstrate diverse application potential across structural engineering, environmental remediation, catalytic reactions, and energy electronics due to the reactivity of their dicarboxyl groups and conjugated double bonds, coupled with the sustainability of their sources. Capable of forming various functional structures such as polyesters, polyamides, MOFs, and metal–organic nanocomposites, they offer pathways for replacing fossil-based materials and developing specialty functional materials.

4.1 Structural materials

Structural materials represent one of the core application areas for MA-based polymers. Leveraging the highly efficient polycondensation reactions of MA carboxyl groups, post-polymerization functionalization modifications, and the unique reactivity of conjugated double bonds, these materials can be tailored to deliver customized properties such as flame retardancy, hydrophobicity, and recyclability. Simultaneously, they maintain excellent mechanical strength, thermal stability, and processability, making them widely applicable in scenarios including engineering plastics, composite materials, and adhesives.

MA undergoes a Diels–Alder cycloaddition reaction to form cyclic dicarboxylic acid derivatives such as cyclohexene dicarboxylic acid, which copolymerizes with hexamethylene diamine and adipic acid to produce modified polyamide (Fig. 10a). Compared to traditional nylon 6,6, these show up to 70% reduced water absorption, doubled char yield, while retaining key mechanical properties. They are suitable for applications requiring high hydrophobicity and flame retardancy, such as automotive and electronic packaging, potentially replacing petroleum-based nylons.[23] The double bond structure of MA allows its direct incorporation into polyester synthesis. For example, copolymerization with butanediol and fumaric acid yielded poly(butanediol muconate-*co*-butanediol fumarate) with molecular weights exceeding 80 kg mol^{-1} and excellent thermomechanical properties, with tensile strength comparable to polyethylene. This material can be used in glass fiber-reinforced composites (*e.g.*, FRP panels) with a shear modulus exceeding 30 GPa, applicable in construction and aerospace (Fig. 10b).[18,20] Using the phospha-Michael addition reaction of the MA derivative *trans*-3-hexenedioic acid (t3HDA), the flame retardant DOPO was covalently grafted onto the nylon-66 backbone, creating intrinsically flame-retardant copolymers. Compared to nylon with physically blended DOPO, these copolymers exhibited a 20% increase in crystallinity, superior thermal stability, a lower fire growth capacity (FGC) index, and better mechanical properties like tensile strength. They are applicable in engineering plastics for the automotive and electronics sectors, requiring flame retardancy (Fig. 10a).[22] Wei *et al.* copolymerized ccMA with various diol diesters, preparing a series of MA-based polyester adhesives. DCP-initiated radical crosslinking formed a dense three-dimensional network, achieving exceptional solvent resistance. After 24 hour immersion in various organic solvents, bond strengths ranged from 0.97 to 4.31 MPa, and after 3 hour immersion in 60 °C water, bond strength remained at 1.09 MPa (Fig. 10c). This work demonstrates the feasibility of utilizing MA as a functional copolymerizable monomer to construct high-performance, crosslinkable polyester adhesives, providing a sustainable and effective strategy for developing high-performance adhesives with strong bonding and solvent durability.[147] Chemically recyclable poly(muconate esters) (polyME) synthesized *via* free radical polymerization, these polymers contain weak C–C bonds in the backbone, enabling efficient depolymerization to monomers (83% recovery) at 258 °C, realizing chemical recycling. Their mechanical properties are tunable (Young's modulus 0.009–1.52 GPa), spanning from brittle to elastomeric ranges. Processable *via* 3D printing, injection molding, and other techniques, it holds promise as a replacement for fossil-based plastics such as polystyrene (PS) and polymethyl methacrylate (PMMA) (Fig. 10d). Technical-economic analysis indicates that production costs can be reduced to \$1.59 kg^{-1} when utilizing recycled monomers, with environmental impacts lower than traditional rubber, aligning with circular economy requirements.[25]

4.2 Environmental materials

Environmental materials focus on the unique physical and chemical properties of MA-based CPs and metal–organic composite particles. Leveraging their fluorescence recognition, photosensitive response, and photocatalytic activity, these materials play a role in environmental remediation scenarios such as heavy metal ion detection, organic wastewater treatment, and organic dye degradation. They exhibit high selectivity, high sensitivity, and environmental adaptability.

Copper ions (Cu^{2+}) are essential trace elements in the human body, but excess amounts can cause diseases like Wilson's disease and Alzheimer's, necessitating the development of highly sensitive and selective materials for Cu^{2+} detection in aqueous media. Biological detection also requires good biocompatibility, which often limits the application of existing CPs due to toxicity or solubility issues. CPs formed from MA derivatives with ions like Zn^{2+} can exhibit strong fluorescence and selectively recognize Cu^{2+} in aqueous solution. For instance, 1D coordination polymers CP1 and CP2 showed highly selective fluorescence quenching towards Cu^{2+} in aqueous media, with a detection limit (LOD) as low as 0.06 μM

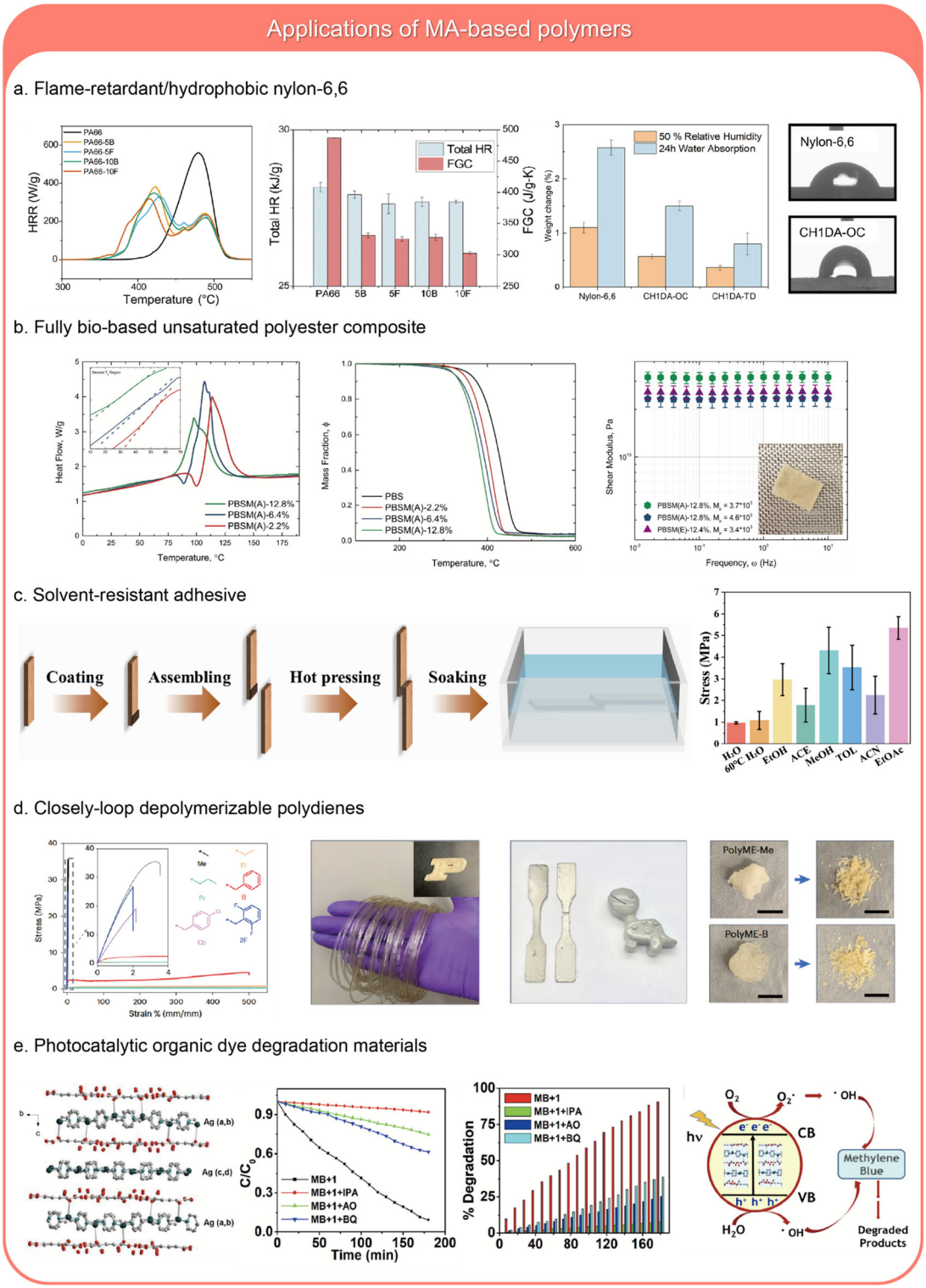

Fig. 10 Applications of MA-based polymers.[18,20,22,23,25,33,147] (a) Flame-retardant/hydrophobic nylon-6,6. Reprinted with permission from Carter *et al.*, *RSC Sustain.*, 2024, **2**, 2968–2978. Copyright © 2024 The Royal Society of Chemistry. Carter *et al.*, *J. Am. Chem. Soc.*, 2022, **144**, 9548–9553. Copyright © 2022 American Chemical Society. Nandi *et al.*, *J. Mol. Struct.*, 2023, **1293**, 136291. Copyright © 2023 Elsevier Science. (b) Fully bio-based unsaturated polyester composite. Reprinted with permission from Rorrer *et al.*, *Green Chem.*, 2017, **19**, 2812–2825. Copyright © 2017 The Royal Society of Chemistry. Rorrer *et al.*, *ACS Sustain. Chem. Eng.*, 2016, **4**, 6867–6876. Copyright © 2016 American Chemical Society. (c) Closely-loop depolymerizable polydienes. Solvent-resistant adhesive. Reprinted with permission from Wei *et al.*, *ACS Sustain. Chem. Eng.*, 2025, **13**, 19136–19144. Copyright © 2025 American Chemical Society. (d) Reprinted with permission from Hu *et al.*, *Nat. Chem. Eng.*, 2025, **2**, 130–141. Copyright © 2025, under exclusive licence to Springer Nature America, Inc. (e) Photocatalytic organic dye degradation materials. Reprinted with permission from Bhunia *et al.*, *New J. Chem.*, 2021, **45**, 13941–13948. Copyright © 2021 The Royal Society of Chemistry.

for CP2, far below WHO and EPA drinking water standards. This makes them suitable for ultratrace Cu^{2+} detection in food, beverages, and biological systems. Furthermore, these CPs can be endocytosed by HepG2 cells, enabling visualization of intracellular Cu^{2+} *via* fluorescence imaging, and showed good biocompatibility at 100 μM concentration (validated by MTT assay), laying the foundation for heavy metal monitoring within biological organisms.[30]

Organic dyes (*e.g.*, methylene blue, MB) are major pollutants in industrial wastewater. Photocatalytic degradation is a green treatment technology, but the efficiency and stability of existing zinc-based CPs need improvement. Three zinc-based CPs were synthesized *via* cooperative coordination of bis(benzimidazole) derivatives (L1/L2) with MA. Structure 1 was a 2D network, 2 a 2D network (forming a 3D supramolecular structure *via* interlayer hydrogen bonds), and 3 a 1D chain (forming a 3D structure *via* hydrogen bonds and aromatic stacking). Under UV light, they exhibited over 90% degradation efficiency for MB, through the synergistic oxidative action of hydroxyl radicals and holes, suitable for organic wastewater treatment.[31] Nandi *et al.* synthesized a 3D silver-based CP *via* an ultrasonic method, featuring a sandwich structure with alternating Ag-bpp cationic chains and 2D water-muconate anionic layers. Under UV light, it achieved 98.06% degradation efficiency for MB (220 min), with a reaction rate constant of 0.0179 min^{-1} (Fig. 10e).[33]

4.3 Energy and electronic materials

Energy and electronic materials utilize MA to produce proton exchange membranes and solid polymer electrolytes. These materials exhibit excellent proton conductivity, lithium ion migration and possess thermal stability and mechanical strength. They provide a bio-based alternative for new energy devices such as fuel cells and lithium-ion batteries, driving green transformation in the energy sector.

Addressing the dependency of commercial polymers on petroleum-based monomers, Carlos Corona-García *et al.* synthesized two types of sulfonated polyamides (MUFABA/MUFASA) with controllable sulfonation degrees *via* polycondensation of MA with fluorinated diamines and sulfonated diamines by adjusting feed ratios. Proton conductivity increased with a higher sulfonation degree. Water uptake (W_u) and ion exchange capacity (IEC) increased with sulfonation degree. MUFASA34 (70.6% sulfonation) achieved a W_u of 36.93% (due to the disulfonate groups in DASDA) and a significantly higher IEC (2.81 meq per g) compared to MUFABA34, inducing phase-separated morphology. Its proton conductivity (σ_p) reached 9.895 mS cm^{-1}, close to other renewable sulfonated polymers. Owing to their renewable origin and good electrochemical performance, these materials show promise for replacing traditional perfluorosulfonic acid membranes (*e.g.*, Nafion) in proton exchange membrane fuel cells (PEMFCs).[21] T. Itoh *et al.* blended lithium polymuconate salt with poly(ethylene oxide) (PEO) or poly(ethylene oxide-*co*-propylene oxide) (P(EO/PO)), adding boron trifluoride diethyl etherate (BF3·OEt2) as a promoter, to prepare solid electrolyte membranes *via* solution casting. Due to the large volume and restricted migration of the polyanion, the lithium ion transference number of these electrolytes reached 0.45–0.88, significantly higher than traditional PEO-$LiN(CF_3SO_2)_2$ electrolytes (0.1–0.14). Similar high lithium ion mobility strategies have also been successfully applied in other renewable material systems, such as cellulose derivatives.[148] The electrochemical stability window was 4.13–4.36 V, and the thermal decomposition temperature exceeded 188 °C. The crystalline polyanion lithium salt acts as a filler, resulting in electrolyte tensile strengths of 6.47–15.54 MPa, markedly higher than traditional electrolytes (0.20–3.55 MPa). These are suitable for high-safety lithium-ion batteries.[149]

4.4 Other materials

Beyond the aforementioned applications, MA-based polymers also find utility in fields such as catalysis and sensing. By regulating the metal coordination state within the material, they offer novel material options for scenarios like photodetector diodes and catalytic reaction carriers, thereby further expanding the application boundaries of MA-based materials.

A 1D nickel coordination polymer synthesized *via in situ* double Michael addition reaction exhibited good stability. It can not only serve as a foundation for novel polymer structures but also be pyrolyzed to prepare carbon-based composite materials loaded with metal nanoparticles like Ni, ZnO, and CoO. NiMucoEtDiPy (using EtDiPy linker) exhibited the largest specific surface area (47.4 m^2 g^{-1}) and pore volume (0.332 cm^3 g^{-1}), significantly higher than CoMuco without a bridging ligand (9.1 m^2 g^{-1}, 0.052 cm^3 g^{-1}), providing efficient precursors for catalysis and adsorption.[34]

In coordination polymers, the structure of water clusters (*e.g.*, cyclic, chain-like) confined within the pores can significantly influence material properties (*e.g.*, adsorption, catalysis), but research on water clusters in muconate-based CPs was previously limited. Simultaneously, the application of CPs in optoelectronics (*e.g.*, Schottky diodes) is still exploratory, requiring the development of muconate CPs with both well-defined structures and excellent photosensitive properties. An Al/CP/FTO device based on a muconate CP with aluminum showed a rectification ratio of 3.668 in the dark, increasing to 5.506 under illumination; specific detectivity reached the 10^9 Jones range, with a photosensitivity of 1.65, consistent with Schottky diode characteristics.[29]

5. Conclusions and future perspectives

MA, a highly promising bio-based monomer derived from renewable resources, holds significant potential for advancing sustainable polymer materials due to its distinctive molecular structure. MA exists in three isomeric forms, each with unique structural features, properties, and polymerization capabilities, dictated by the configuration of its conjugated double bonds. Additionally, MA can be readily functionalized into esters and

ammonium salts, broadening its versatility for tailored applications. Currently, MA is produced *via* two primary routes: chemical conversion and biological fermentation. Compared to conventional chemical methods, biological fermentation offers notable advantages, including environmentally friendly, flexible feedstock utilization, and higher product purity. MA-based polymers can be synthesized through diverse polymerization strategies, including polycondensation *via* dicarboxylic acid groups, addition polymerization across conjugated double bonds, and coordination polymerization with metal ions. Such approaches enable the production of a wide range of functional materials, such as unsaturated polyester, polyamides, and coordination polymers. These materials exhibit outstanding performance across structural, environmental, energy, and electronic applications—examples include heavy metal detection, optical sensing, flame retardant modification, proton conduction. Beyond renewable sourcing, achieving true materials circularity requires end-of-life strategies that enable repair, reprocessing, and/or closed-loop recycling without sacrificing performance. Dynamic covalent chemistry provides a general framework to couple sustainable feedstocks with intrinsic recyclability by integrating reversible bond-exchange motifs into polymer backbones or networks. For MA-derived polymers, the conjugated diene and dicarboxylate functionalities offer versatile handles to introduce such dynamic motifs and thus design circular polymer systems.[150,151] Collectively, MA-based polymers provide a compelling pathway toward replacing petroleum-derived polymers and promoting sustainable development.

Currently, the advancement of MA-based polymers faces several interconnected challenges that hinder their widespread adoption. Although the biotechnological routes, such as microbial fermentation, provide an environmentally friendly alternative, their efficiency is constrained by low metabolic flux and limited yields. Furthermore, issues of microbial toxicity toward key substrates such as vanillin and catechol remain unresolved. This necessitates the development of more tolerant microbial strains and optimized feedstocks. From a synthesis standpoint, biorefinery approaches currently yield only the ccMA isomer, while the ttMA variant requires additional chemical isomerization—a process that introduces complexity. The inherent physicochemical properties of MA and its isomers, such as their high melting points and poor solubility in common organic solvents, further complicate direct polymerization. Although chemical derivatization can enhance monomer solubility and processability, it often involves extra synthetic steps, thereby reducing overall atom economy. Moreover, specialized techniques such as topological polymerization require precise and stringent conditions that are difficult to up for industrial production. In terms of material performance, many MA-based polymers still lag behind conventional petroleum-derived counterparts in mechanical robustness and thermal stability. Coordination polymers derived from MA also face challenges related to long-term stability and cost-effective production. Moreover, the current number of published life cycle assessment case studies on polymer systems derived from MA remains relatively limited, highlighting the need to establish a unified benchmark assessment system for comparison with petroleum-based conventional products. Collectively, these limitations impede the transition of MA-based polymers from laboratory curiosities to commercially viable materials.

To address these barriers and propel the field forward, the following strategic directions are proposed: (i) Advancement of biosynthetic platforms: leverage synthetic biology tools, including gene editing and metabolic pathway engineering, to enhance microbial tolerance and increase fermentation titers. Concurrently, explore novel and sustainable feedstocks—such as industrial biowastes—to develop efficient conversion pathways, thereby reducing production costs and accelerating industrial scalability. (ii) Innovation in monomer and polymer design: develop novel derivative strategies to improve monomer solubility and reactivity without significantly increasing synthetic complexity. Optimize polymerization techniques—including topological and bulk polymerization—to achieve high stereoregularity and controlled architectures. Integrate computational and AI-assisted methods for precise molecular design and to tailor polymer properties for specific applications. (iii) Expansion into high-performance applications: exploit the tunable functionality and inherent degradability of MA-based polymers to engineer advanced materials for high-value sectors. By tailoring their chemical and physical properties, these sustainable polymers can replace petroleum-based counterparts in specialized applications such as biomedical devices, high-barrier packaging, and functional coatings. (iv) Fostering cross-disciplinary collaboration: accelerating progress in this field will require sustained and structured collaboration across disciplines—including microbiology, chemistry, materials science, and chemical engineering. Such integrative efforts are essential to generate disruptive ideas and achieve breakthrough innovations that can overcome existing technical bottlenecks and unlock new application landscapes. Together, these approaches form a cohesive roadmap toward realizing the full potential of MA-based polymers as sustainable, high-performance materials of the future.

Conflicts of interest

There are no conflicts to declare.

Data availability

Data are provided within the manuscript. No primary research results, software or code have been included, and no new data were generated or analysed as part of this review.

Acknowledgements

This work was supported by the National Natural Science Foundation of China (32271972), 5·5 Engineering Research &

Innovation Team Project of Beijing Forestry University (No. BLRC 2023B05), and the Natural Science Foundation of Tianjin (24JCJQJC00030). Additionally, the authors appreciate the assistance of the Innovation Platform for High Value Utilization of Forest Resources at Beijing Forestry University.

References

1 Q. Zhang, M. Song, Y. Xu, W. Wang, Z. Wang and L. Zhang, Bio-based polyesters: Recent progress and future prospects, *Prog. Polym. Sci.*, 2021, **120**, 101430.
2 D. K. Schneiderman and M. A. Hillmyer, 50th anniversary perspective: there is a great future in sustainable polymers, *Macromolecules*, 2017, **50**, 3733–3749.
3 Y. Zhu, C. Romain and C. K. Williams, Sustainable polymers from renewable resources, *Nature*, 2016, **540**, 354–362.
4 A. Gandini and T. M. Lacerda, From monomers to polymers from renewable resources: recent advances, *Prog. Polym. Sci.*, 2015, **48**, 1–39.
5 R. Hatti-Kaul, L. J. Nilsson, B. Zhang, N. Rehnberg and S. Lundmark, Designing biobased recyclable polymers for plastics, *Trends Biotechnol.*, 2020, **38**, 50–67.
6 M. Rujnić-Sokele and A. Pilipović, Challenges and opportunities of biodegradable plastics: A mini review, *Waste Manag. Res.*, 2017, **35**, 132–140.
7 Y. Zhang, Q. Lei, R. Liu, L. Zhang, B. Lyu, L. Liu and J. Ma, Self-healing cellulose-based flexible sensor: a review, *Ind. Crops Prod.*, 2023, **206**, 117724.
8 R. M. Cywar, N. A. Rorrer, C. B. Hoyt, G. T. Beckham and E. Y.-X. Chen, Bio-based polymers with performance-advantaged properties, *Nat. Rev. Mater.*, 2021, **7**, 83–103.
9 Z. Wang, M. S. Ganewatta and C. Tang, Sustainable polymers from biomass: Bridging chemistry with materials and processing, *Prog. Polym. Sci.*, 2020, **101**, 101197.
10 M. Jaffé, Über die aufspaltung des benzolrings im organismus. I. Mitteilung. Das auftreten von muconsäure im harn nach darreichung von benzol, *Hoppe Seylers Z. Physiol. Chem.*, 1909, **62**, 58–67.
11 I. Khalil, G. Quintens, T. Junkers and M. Dusselier, Muconic acid isomers as platform chemicals and monomers in the biobased economy, *Green Chem.*, 2020, **22**, 1517–1541.
12 H. Yang, X. Lin, X. Zhong, M. Cao, J. Yuan, Z. Li, X. Ling and N. He, Current status and advances in the green synthesis of muconic acid, *Crit. Rev. Biotechnol.*, 2024, **45**, 1–18.
13 S. Choi, H.-N. Lee, E. Park, S.-J. Lee and E.-S. Kim, Recent advances in microbial production of cis,cis-muconic acid, *Biomolecules*, 2020, **10**, 1238.
14 N.-Z. Xie, H. Liang, R.-B. Huang and P. Xu, Biotechnological production of muconic acid: current status and future prospects, *Biotechnol. Adv.*, 2014, **32**, 615–622.
15 J. E. Matthiesen, J. M. Carraher, M. Vasiliu, D. A. Dixon and J.-P. Tessonnier, Electrochemical conversion of muconic acid to biobased diacid monomers, *ACS Sustainable Chem. Eng.*, 2016, **4**, 3575–3585.
16 S. Capelli, A. Rosengart, A. Villa, A. Citterio, A. D. Michele, C. L. Bianchi, L. Prati and C. Pirola, Bio-adipic acid production by catalysed hydrogenation of muconic acid in mild operating conditions, *Appl. Catal., B*, 2017, **218**, 220–229.
17 S. Zhang, Q. Li, K. He, Z. Cui, X. Sheng, Y. Zhu and T. Tan, Computational redesign of an enoate reductase for the in vivo production of adipic acid from muconic acid, *Chem Catal.*, 2024, **4**, 101042.
18 N. A. Rorrer, D. R. Vardon, J. Dorgan, E. Gjersing and G. Beckham, Biomass-derived monomers for performance-differentiated fiber reinforced polymer composites, *Green Chem.*, 2017, **19**, 2812–2825.
19 Y. Yu, H. Xiong, J. Xiao, X. Qian, X. Leng, Z. Wei and Y. Li, High molecular weight unsaturated copolyesters derived from fully biobased *trans*-β-hydromuconic acid and fumaric acid with 1,4-butanediol: synthesis and thermomechanical properties, *ACS Sustainable Chem. Eng.*, 2019, **7**, 6859–6869.
20 N. A. Rorrer, J. R. Dorgan, D. R. Vardon, C. R. Martinez, Y. Yang and G. T. Beckham, Renewable unsaturated polyesters from muconic acid, *ACS Sustainable Chem. Eng.*, 2016, **4**, 6867–6876.
21 C. Corona-García, A. Onchi, A. A. Santiago, T. E. Soto, S. R. Vasquez-Garcia, D. Pacheco-Catalán and J. Vargas, Synthesis, characterization, and proton conductivity of muconic acid-based polyamides bearing sulfonated moieties, *Polymers*, 2023, **15**, 4499.
22 P. Carter, P. M. Meyer, T.-H. Lee, D. Dileep, N. L. Chalgren, S. Noreen, M. J. Forrester, B. H. Shanks, J.-P. Tessonnier and E. W. Cochran, Leveraging the bio-enabled muconic acid platform via phospha-michael-addition: intrinsically flame-retardant nylon-66/DOPO copolymers, *RSC Sustainability*, 2024, **2**, 2968–2978.
23 P. Carter, J. L. Trettin, T.-H. Lee, N. L. Chalgren, M. J. Forrester, B. Shanks, J. Tessonnier and E. W. Cochran, Bioenabled platform to access polyamides with built-In target properties, *J. Am. Chem. Soc.*, 2022, **144**, 9548–9553.
24 A. Matsumoto, T. Matsumura and S. Aoki, Stereospecific polymerization of dialkyl muconates through free radical polymerization: isotropic polymerization and topochemical polymerization, *Macromolecules*, 1996, **29**, 423–432.
25 Q. Hu, X. Luo, L. A. Ogunfowora, A. Athaley, J. S. DesVeaux, B. C. Klein, S. Xu, P. Wu, Z. Wei, C. Lin, T. Haraniya, D. Maiorano, B. Boudouris, J. Mei, M. Urgun-Demirtas, G. T. Beckham, B. M. Savoie and L. Dou, Scalable, biologically sourced depolymerizable polydienes with intrinsically weakened carbon–carbon bonds, *Nat. Chem. Eng.*, 2025, **2**, 130–141.
26 Y. Bando, T. Dodou and Y. Minoura, Radical polymerization of muconic acid and ethyl muconate, *J. Polym. Sci., Polym. Chem. Ed.*, 1977, **15**, 1917–1926.
27 G. Quintens, J. H. Vrijsen, P. Adriaensens, D. Vanderzande and T. Junkers, Muconic acid esters as bio-based acrylate mimics, *Polym. Chem.*, 2019, **10**, 5555–5563.

28 X. Luo, Z. Wei, B. Seo, Q. Hu, X. Wang, J. A. Romo, M. Jain, M. Cakmak, B. W. Boudouris, K. Zhao, J. Mei, B. M. Savoie and L. Dou, Circularly recyclable polymers featuring topochemically weakened carbon–carbon bonds, *J. Am. Chem. Soc.*, 2022, **144**, 16588–16597.
29 F. Ahmed, J. Datta, S. Sarkar, B. Dutta, A. D. Jana, P. Ray and M. H. Mir, Water tetramer confinement and photosensitive schottky behavior of a 2D coordination polymer, *Chemistryselect*, 2018, **3**, 6985–6991.
30 S. Bhunia, B. Dutta, K. Pal, A. Chandra, K. Jana and C. Sinha, Ultra-trace level detection of Cu^{2+} in an aqueous medium by novel Zn(ii)-dicarboxylato–pyridyl coordination polymers and cell imaging with HepG2 cells, *New J. Chem.*, 2021, **45**, 13941–13948.
31 X. Wei, Z.-C. Hao, C. Han and G. Cui, Syntheses, crystal structures and photocatalytic properties of three zinc(II) coordination polymers constructed by mixed ligands, *J. Mol. Struct.*, 2020, **1200**, 127117.
32 R. K. Baimuratova, G. I. Dzhardimalieva, N. D. Golubeva, N. N. Dremova and A. V. Ivanov, Coordination polymers based on *trans*,*trans* -muconic acid: synthesis, structure, adsorption and thermal properties, *Pure Appl. Chem.*, 2020, **92**, 859–870.
33 L. Nandi, S. Barman, A. Das, P. Brandão, E. Zangrando, A. Basu and S. Dalai, 3D Ag(I) coordination polymer sandwiched by water-muconate anionic layers: synthesis, structure, hirshfeld surface analysis, binding with BSA, and photocatalytic activity, *J. Mol. Struct.*, 2023, **1293**, 136291.
34 J. Do, J. Kang, Y. Jung, Y. S. Park and A. J. Jacobson, 1D nickel coordination polymers with an unnatural amino acid prepared by *in situ* double michael addition of ethylenediamine to (*E*,*E*)–muconic acid, *Bull. Korean Chem. Soc.*, 2017, **38**, 1507–1510.
35 A. Matsumoto, T. Tanaka, T. Tsubouchi, K. Tashiro, S. Saragai and S. Nakamoto, Crystal engineering for topochemical polymerization of muconic esters using halogen–halogen and CH/π interactions as weak intermolecular interactions, *J. Am. Chem. Soc.*, 2002, **124**, 8891–8902.
36 A. Matsumoto, T. Odani, M. Chikada, K. Sada and M. Miyata, Crystal-lattice controlled photopolymerization of di(benzylammonium) (Z,Z)-muconates, *J. Am. Chem. Soc.*, 1999, **121**, 11122–11129.
37 A. Matsumoto, T. Odani, K. Sada, M. Miyata and K. Tashiro, Intercalation of alkylamines into an organic polymer crystal, *Nature*, 2000, **405**, 328–330.
38 B. H. Shanks and P. L. Keeling, Bioprivileged molecules: creating value from biomass, *Green Chem.*, 2017, **19**, 3177–3185.
39 D. M. Patel, P. T. Prabhu, G. Gupta, M. N. Dell'Anna, S. Kling, H. T. Nguyen, J.-P. Tessonnier and L. T. Roling, Structure sensitivity of the electrochemical hydrogenation of cis,cis-muconic acid to hexenedioic acid and adipic acid, *Green Chem.*, 2024, **26**, 4506–4517.
40 C. Ver Elst, R. Vroemans, M. Bal, S. Sergeyev, C. Mensch and B. U. W. Maes, Synthesis of levulinic acids from muconic acids in hot water, *Angew. Chem., Int. Ed.*, 2023, **62**, e202309597.
41 R. Lu, F. Lu, J. Chen, W. Yu, Q. Huang, J. Zhang and J. Xu, Production of diethyl terephthalate from biomass–derived muconic acid, *Angew. Chem., Int. Ed.*, 2015, **55**, 249–253.
42 A. Matsumoto, T. Odani and S. Aoki, Stereoregular photopolymerization of di(benzylammonium) muconate in the crystalline state, *Polym. J.*, 1998, **30**, 358–360.
43 A. Matsumoto, K. Katayama, T. Odani, K. Oka, K. Tashiro, S. Saragai and S. Nakamoto, Feature of γ-radiation polymerization of muconic acid derivatives in the crystalline state, *Macromolecules*, 2000, **33**, 7786–7792.
44 T. Odani and A. Matsumoto, First example of the topochemical polymerization of the (E,E)-muconic acid derivative, *Macromol. Rapid Commun.*, 2000, **21**, 40–44.
45 A. Matsumoto and T. Odani, Topochemical polymerization of 1,3-diene monomers and features of polymer crystals as organic intercalation materials, *Macromol. Rapid Commun.*, 2001, **22**, 1195.
46 S. Saragai, K. Tashiro, S. Nakamoto, T. Kamae, A. Matsumoto and T. Tsubouchi, Comparison of crystal structure between low- and high-temperature phases of diethyl (Z,Z)-muconate. A trial to investigate the reasons why the solid-state polymerization reaction is ceased at low temperature, *Polym. J.*, 2001, **33**, 199–203.
47 S. Saragai, K. Tashiro, S. Nakamoto, A. Matsumoto and T. Tsubouchi, Relationship between packing structure and monomer reactivity in the photoinduced solid-state polymerizations of muconic diesters with different side groups, *J. Phys. Chem. B*, 2001, **105**, 4155–4165.
48 A. Matsumoto, S. Oshita and D. Fujioka, A novel organic intercalation system with layered polymer crystals as the host compounds derived from 1,3-diene carboxylic acids, *J. Am. Chem. Soc.*, 2002, **124**, 13749–13756.
49 S. Nagahama and A. Matsumoto, Thermally induced topochemical polymerization of 1,3-diene monomers, *Chem. Lett.*, 2002, **31**, 1026–1027.
50 T. Odani and A. Matsumoto, Solvent-free synthesis of layered polymer crystals, *Polym. J.*, 2002, **34**, 841–846.
51 T. Tanaka and A. Matsumoto, First disyndiotactic polymer from a 1,4-disubstituted butadiene by alternate molecular stacking in the crystalline state, *J. Am. Chem. Soc.*, 2002, **124**, 9676–9677.
52 K. Tashiro, S. Nakamoto, T. Fujii and A. Matsumoto, Generation and relaxation of large stress in the photoinduced solid-state polymerization reaction of diethyl muconate detected by simultaneous time-resolved measurement of X-ray diffraction and raman spectra, *Polymer*, 2003, **44**, 6043–6049.
53 A. Matsumoto, D. Fujioka and T. Kunisue, Organic intercalation of unsaturated amines into layered polymer crystals and solid-state photoreactivity of the guest molecules in constrained interlayers, *Polym. J.*, 2003, **35**, 652–661.
54 S. Nakamoto, K. Tashiro and A. Matsumoto, Quantitative evaluation of stress distribution in bulk polymer samples through the comparison of mechanical behaviors between

giant single–crystal and semicrystalline samples of poly (trans–1,4-diethyl muconate), *J. Polym. Sci., Polym. Chem. Ed.*, 2003, **41**, 444–453.
55 S. Nakamoto, K. Tashiro and A. Matsumoto, Vibrational spectroscopic study on the molecular deformation mechanism of a poly(*trans*-1,4-diethyl muconate) single crystal subjected to tensile stress, *Macromolecules*, 2003, **36**, 109–117.
56 S. Nagahama and A. Matsumoto, Two–dimensional polymer synthesis through the topochemical polymerization of alkylenediammonium muconate as a multifunctional monomer, *J. Polym. Sci., Polym. Chem. Ed.*, 2004, **42**, 3922–3929.
57 S. Oshita, T. Tanaka and A. Matsumoto, Synthesis of new stereoregular host polymers for organic intercalation by solid-state hydrolysis using layered syndiotactic polymer crystals, *Chem. Lett.*, 2005, **34**, 1442–1443.
58 A. Matsumoto, D. Furukawa and H. Nakazawa, Stereocontrol of diene polymers by topochemical polymerization of substituted benzyl muconates and their crystallization properties, *J. Polym. Sci., Polym. Chem. Ed.*, 2006, **44**, 4952–4965.
59 A. Matsumoto, D. Furukawa, Y. Mori, T. Tanaka and K. Oka, Change in crystal structure and polymerization reactivity for the solid-state polymerization of muconic esters, *Cryst. Growth Des.*, 2007, **7**, 1078–1085.
60 D. Furukawa and A. Matsumoto, Reaction mechanism based on X-ray crystal structure analysis during the solid-state polymerization of muconic esters, *Macromolecules*, 2007, **40**, 6048–6056.
61 Y. Mori and A. Matsumoto, Molecular stacking and photoreactions of fluorine-substituted benzyl muconates in the crystals, *Cryst. Growth Des.*, 2007, **7**, 377–385.
62 T. Ueno, D. Furukawa and A. Matsumoto, Thermally induced polymerization of muconic esters in the solid state studied by infrared microscope spectroscopy under temperature control, *Macromol. Chem. Phys.*, 2008, **209**, 357–365.
63 K. Onodera, C. Tanioku and A. Matsumoto, Epitaxial crystal growth and solid-state polymerization of piperonyl muconate on the {001} surface of KCl crystal for controlling polymer chain alignment, *ACS Appl. Mater. Interfaces*, 2012, **4**, 2280–2287.
64 S. Usukawa, A. Matsumoto and Y. Suzuki, Exceptionally high melting temperature of polymer crystal with fully extended chains prepared via topochemical polymerization and its analysis based on nonlinear modified hoffman–weeks approach, *Macromolecules*, 2025, **58**, 5738–5746.
65 E. H. Farmer, CCXCI.—muconic and hydromuconic acids. Part II. The isomerism of the muconic acids, *J. Chem. Soc. Trans.*, 1923, **123**, 2531–2548.
66 S. Scelfo, R. Pirone and N. Russo, Solubility of cis, cis-muconic acid in various polar solvents from 298.15 K to 348.15 K, *Iran. J. Chem. Chem. Eng.*, 2017, **36**, 129–136.
67 J. Gorden, T. Zeiner, G. Sadowski and C. Brandenbusch, Recovery of cis,cis-muconic acid from organic phase after reactive extraction, *Sep. Purif. Technol.*, 2016, **169**, 1–8.
68 M. N. Dell'Anna, M. Laureano, H. Bateni, J. E. Matthiesen, L. Zaza, M. P. Zembrzuski, T. J. Paskach and J.-P. Tessonnier, Electrochemical hydrogenation of bioprivilegedcis,cis-muconic acid totrans-3-hexenedioic acid: from lab synthesis to bench-scale production and beyond, *Green Chem.*, 2021, **23**, 6456–6468.
69 D. N. Zakusilo, E. I. Evstigneyev, A. Y. Ivanov, A. S. Mazur, E. A. Bessonova, O. A. Mammeri and A. V. Vasilyev, Structure of oxidized hydrolysis lignin, *J. Wood Chem. Technol.*, 2023, **43**, 103–115.
70 M. Kohlstedt, S. Starck, N. Barton, J. Stolzenberger, M. Selzer, K. Mehlmann, R. Schneider, D. Pleissner, J. Rinkel, J. S. Dickschat, J. Venus, J. B. J. H. van Duuren and C. Wittmann, From lignin to nylon: cascaded chemical and biochemical conversion using metabolically engineered *pseudomonas putida*, *Metab. Eng.*, 2018, **47**, 279–293.
71 A. E. Settle, L. Berstis, S. Zhang, N. A. Rorrer, H. Hu, R. M. Richards, G. T. Beckham, M. F. Crowley and D. R. Vardon, Iodine-catalyzed isomerization of dimethyl muconate, *ChemSusChem*, 2018, **11**, 1768–1780.
72 J. M. Carraher, P. Carter, R. G. Rao, M. J. Forrester, T. Pfennig, B. H. Shanks, E. W. Cochran and J.-P. Tessonnier, Solvent-driven isomerization of cis,cis-muconic acid for the production of specialty and performance-advantaged cyclic biobased monomers, *Green Chem.*, 2020, **22**, 6444–6454.
73 I. Khalil, F. Rammal, L. D. Vriendt, A. S. Narmon, B. F. Sels, S. Meier and M. Dusselier, Solvent-driven isomerization of muconates in DMSO: reaction mechanism and process sustainability, *Green Chem.*, 2024, **26**, 5852–5861.
74 I. Khalil, M. G. Rigamonti, K. Janssens, A. Bugaev, E. D. Arenas, S. Robijns, T. Donckels, M. T. Beydokhti, S. Bals, D. E. De Vos and M. Dusselier, Atomically dispersed ruthenium hydride on beta zeolite as catalysts for the isomerization of muconates, *Nat. Catal.*, 2024, **7**, 921–933.
75 J. A. Elvidge, R. P. Linstead, P. Sims and B. A. Orkin, 462. The third isomeric (cis-trans-) muconic acid, *J. Chem. Soc.*, 1950, 2235.
76 J. W. Jaroszewski and M. G. Ettlinger, 1,3-butadiene-1,1,4-tricarboxylic acids, *J. Org. Chem.*, 1982, **47**, 3974–3976.
77 A. C. Blaga, D. G. Gal and A. Tucaliuc, Recent advances in muconic acid extraction process, *Appl. Sci.*, 2023, **13**, 11691.
78 J. W. Frost, A. Miermont, D. Schweitzer, V. Bui and E. Lansing, *Preparation of Trans, Trans Muconic Acid and Trans, Trans Muconates*, 2010, US20100314243A1.
79 N. S. Kruyer, N. Wauldron, A. S. Bommarius and P. Peralta-Yahya, Fully biological production of adipic acid analogs from branched catechols, *Sci. Rep.*, 2020, **10**, 1–8.

80 H. Almqvist, H. Veras, K. Li, J. G. Hidalgo, C. Hulteberg, M. Gorwa-Grauslund, N. S. Parachin and M. Carlquist, Muconic acid production using engineered pseudomonas putida KT2440 and a guaiacol-rich fraction derived from kraft lignin, *ACS Sustainable Chem. Eng.*, 2021, **9**, 8097–8106.

81 M. Giurg, E. Kowal, H. Muchalski, L. Syper and J. Młochowski, Catalytic oxidative domino degradation of alkyl phenols towards 2- and 3-substituted muconolactones, *Synth. Commun.*, 2008, **39**, 251–266.

82 A. J. Zaczek and T. M. Korter, Polymorphism in cis–trans muconic acid crystals and the role of C–H···O hydrogen bonds, *Cryst. Growth Des.*, 2017, **17**, 4458–4466.

83 B. Briou, B. Améduri and B. Boutevin, Trends in the diels–alder reaction in polymer chemistry, *Chem. Soc. Rev.*, 2021, **50**, 11055–11097.

84 P. Wu, Q. Hu, A. V. Marquardt, L. A. Ogunfowora, J. H. Kim, Y. Tang, C. Lin, B. M. Savoie and L. Dou, Photoinduced bulk polymerization strategy in melt state for recyclable polydiene derivatives, *Nat. Chem.*, 2025, **17**, 1091–1098.

85 P. C. Guha and D. K. Sankaran, Muconic acid, *Org. Synth.*, 1946, **26**, 57.

86 A. J. Pandell, Enzymic-like aromatic oxidations. Metal-catalyzed peracetic acid oxidation of phenol and catechol to *cis*,*cis*-muconic acid, *J. Org. Chem.*, 1976, **41**, 3992–3996.

87 J. Tsuji and H. Takayanagi, Oxidative cleavage reactions of catechol and phenol to monoester of *cis*,*cis*-muconic acid with the oxidizing systems of O_2/CuCl, KOH/$CuCl_2$, *Tetrahedron*, 1978, **34**, 641–644.

88 A. B. McKague, Synthesis of muconic acids by peracetic acid oxidation of catechols, *Synth. Commun.*, 1999, **29**, 1463–1475.

89 G. M. S. R. O. Rocha, R. A. W. Johnstone and M. G. P. M. S. Neves, Catalytic effects of metal(IV) phosphates on the oxidation of phenol and 2-naphthol, *J. Mol. Catal. A:Chem.*, 2002, **187**, 95–104.

90 F. Coupé, L. Petitjean, P. T. Anastas, F. Caijo, V. Escande and C. Darcel, Sustainable oxidative cleavage of catechols for the synthesis of muconic acid and muconolactones including lignin upgrading, *Green Chem.*, 2020, **22**, 6204–6211.

91 B. Hočevar, A. Prašnikar, M. Huš, M. Grilc and B. Likozar, H_2-free Re–based catalytic dehydroxylation of aldaric acid to muconic and adipic acid esters, *Angew. Chem., Int. Ed.*, 2020, **60**, 1244–1253.

92 K. Katayama, H. Hotta and Y. Tsujino, Efficient synthesis of *cis*,*cis*-muconic acid by catechol oxidation of ozone in the presence of a base, *Molecules*, 2025, **30**, 201.

93 G. O. Rocha, J. Rocha and Z. Lin, Study of Catalyst Selectivity in the Oxidation of Phenol, *Catal. Lett.*, 2003, **89**, 69–74.

94 S. G. Van Ornum, R. M. Champeau and R. Pariza, Ozonolysis applications in drug synthesis, *Chem. Rev.*, 2006, **106**, 2990–3001.

95 M. Kooti and M. Jorfi, Mild and efficient oxidation of aromatic alcohols and other substrates using NiO_2 /CH_3 COOH system, *J. Chem.*, 2007, **5**, 365–369.

96 R. Fujiwara, S. Noda, T. Tanaka and A. Kondo, Muconic acid production using gene-level fusion proteins in escherichia coli, *ACS Synth. Biol.*, 2018, **7**, 2698–2705.

97 J. Becker, M. Kuhl, M. Kohlstedt, S. Starck and C. Wittmann, Metabolic engineering of corynebacterium glutamicum for the production of cis, cis-muconic acid from lignin, *Microb. Cell Fact.*, 2018, **17**, 115.

98 M. Li, J. Chen, K. He, C. Su, Y. Wu and T. Tan, Corynebacterium glutamicum cell factory design for the efficient production of cis, cis-muconic acid, *Metab. Eng.*, 2024, **82**, 225–237.

99 X.-Y. Ye, Q. Sun, H.-J. Huang, X.-F. Cao, L. Zhang and T.-Q. Yuan, Unveiling the structural characteristics of acetone-insoluble substances in various cellulose diacetate, *Carbohydr. Polym.*, 2025, **360**, 123616.

100 Q. Sun, W.-J. Chen, B. Pang, Z. Sun, S. S. Lam, C. Sonne and T.-Q. Yuan, Ultrastructural change in lignocellulosic biomass during hydrothermal pretreatment, *Bioresour. Technol.*, 2021, **341**, 125807.

101 X. Chen, L. Zhou, K. Tian, A. Kumar, S. Singh, B. A. Prior and Z. Wang, Metabolic engineering of *escherichia coli*: a sustainable industrial platform for bio-based chemical production, *Biotechnol. Adv.*, 2013, **31**, 1200–1223.

102 M. Ikeda, Towards bacterial strains overproducing l-tryptophan and other aromatics by metabolic engineering, *Appl. Microbiol. Biotechnol.*, 2006, **69**, 615–626.

103 S. Ghosh, Y. Chisti and U. C. Banerjee, Production of shikimic acid, *Biotechnol. Adv.*, 2012, **30**, 1425–1431.

104 C. Ling, G. L. Peabody, D. Salvachúa, Y.-M. Kim, C. M. Kneucker, C. H. Calvey, M. A. Monninger, N. M. Munoz, B. C. Poirier, K. J. Ramirez, P. C. St. John, S. P. Woodworth, J. K. Magnuson, K. E. Burnum-Johnson, A. M. Guss, C. W. Johnson and G. T. Beckham, Muconic acid production from glucose and xylose in pseudomonas putida via evolution and metabolic engineering, *Nat. Commun.*, 2022, **13**, 4925.

105 H.-M. Jung, M.-Y. Jung and M.-K. Oh, Metabolic engineering of klebsiella pneumoniae for the production of cis,cis-muconic acid, *Appl. Microbiol. Biotechnol.*, 2015, **99**, 5217–5225.

106 H.-N. Lee, W.-S. Shin, S.-Y. Seo, S.-S. Choi, J. Song, J. Kim, J.-H. Park, D. Lee, S. Y. Kim, S. J. Lee, G.-T. Chun and E.-S. Kim, Corynebacterium cell factory design and culture process optimization for muconic acid biosynthesis, *Sci. Rep.*, 2018, **8**, 18041.

107 C. R. Amendola, W. T. Cordell, C. M. Kneucker, C. J. Szostkiewicz, M. A. Ingraham, M. Monninger, R. Wilton, B. F. Pfleger, D. Salvachúa, C. W. Johnson and G. T. Beckham, Comparison of wild-type KT2440 and genome-reduced EM42 *Pseudomonas putida* strains for muconate production from aromatic compounds and glucose, *Metab. Eng.*, 2024, **81**, 88–99.

108 M. Suástegui, C. Y. Ng, A. Chowdhury, W. Sun, M. Cao, E. House, C. D. Maranas and Z. Shao, Multilevel engineering of the upstream module of aromatic amino acid biosynthesis in *Saccharomyces cerevisiae* for high production of polymer and drug precursors, *Metab. Eng.*, 2017, **42**, 134–144.

109 G. Wang, S. Øzmerih, R. Guerreiro, A. C. Meireles, A. Carolas, N. Milne, M. K. Jensen, B. S. Ferreira and I. Borodina, Improvement of cis,cis-muconic acid production in saccharomyces cerevisiae through biosensor-aided genome engineering, *ACS Synth. Biol.*, 2020, **9**, 634–646.

110 T. Nicolaï, Q. Deparis, M. R. Foulquié-Moreno and J. M. Thevelein, *In situ* muconic acid extraction reveals sugar consumption bottleneck in a xylose-utilizing saccharomyces cerevisiae strain, *Microb. Cell Fact.*, 2021, **20**, 114.

111 M. E. Pyne, J. A. Bagley, L. Narcross, K. Kevvai, K. Exley, M. Davies, Q. Wang, M. Whiteway and V. J. J. Martin, Screening non-conventional yeasts for acid tolerance and engineering pichia occidentalis for production of muconic acid, *Nat. Commun.*, 2023, **14**, 5294.

112 K. A. Curran, J. M. Leavitt, A. S. Karim and H. S. Alper, Metabolic engineering of muconic acid production in *saccharomyces cerevisiae*, *Metab. Eng.*, 2013, **15**, 55–66.

113 C. Weber, C. Brückner, S. Weinreb, C. Lehr, C. Essl and E. Boles, Biosynthesis of *cis*,*cis*-muconic acid and its aromatic precursors, catechol and protocatechuic acid, from renewable feedstocks by saccharomyces cerevisiae, *Appl. Environ. Microbiol.*, 2012, **78**, 8421–8430.

114 S.-S. Choi, S.-Y. Seo, S.-O. Park, H.-N. Lee, J. Song, J. Kim, J.-H. Park, S. Kim, S. J. Lee, G.-T. Chun and E.-S. Kim, Cell factory design and culture process optimization for dehydroshikimate biosynthesis in escherichia coli, *Front. Bioeng. Biotechnol.*, 2019, **7**, 241.

115 J. Fernández-Rodríguez, X. Erdocia, C. Sánchez, A. M. González and J. Labidi, Lignin depolymerization for phenolic monomers production by sustainable processes, *J. Energy Chem.*, 2017, **26**, 622–631.

116 X.-Y. Ye, X.-Y. Hui, Q. Sun, C. Zhang, S. Hong, J.-L. Wen and T.-Q. Yuan, A mild process for producing high-performance dissolving pulp toward highly-substituted cellulose acetate: integrated production of lignin nanoparticles and closed-loop solvent recycling, *Green Chem.*, 2026, **28**, 1127–1143.

117 Y. Chen, B. Fu, G. Xiao, L.-Y. Ko, T.-Y. Kao, C. Fan and J. Yuan, Bioconversion of lignin-derived feedstocks to muconic acid by whole-cell biocatalysis, *ACS Food Sci. Technol.*, 2021, **1**, 382–387.

118 L. T. Nguyen, D.-P. Phan, A. Sarwar, M. H. Tran, O. K. Lee and E. Y. Lee, Valorization of industrial lignin to value-added chemicals by chemical depolymerization and biological conversion, *Ind. Crops Prod.*, 2021, **161**, 113219.

119 W. Zhang, G. Wang, B. Zhang, W. Sui, C. Si, L. Zhou and H. Jia, Green potassium fertilizer from enzymatic hydrolysis lignin: Effects of lignin fractionation on wheat seed germination and seedling growth, *Int. J. Biol. Macromol.*, 2024, **262**, 130017.

120 X. Shen, Z. Zhao, J. Wen, J. Zhang, Y. Ji, G. Hou, Y. Liao, C. Zhang, T.-Q. Yuan and F. Wang, Standardization transformation of C-lignin to catechol and propylene, *Nat. Commun.*, 2025, **16**, 6245.

121 Z.-H. Zhang, X. Wu, X. Ren, Z. Rong, Z. Sun, K. Barta and T.-Q. Yuan, High yield production of 1,4-cyclohexanediol from lignin derived 2,6-dimethoxybenzoquinone via raney NiMn catalyst in hydrogen free conditions, *J. Energy Chem.*, 2023, **83**, 275–286.

122 N. Barton, L. Horbal, S. Starck, M. Kohlstedt, A. Luzhetskyy and C. Wittmann, Enabling the valorization of guaiacol-based lignin: integrated chemical and biochemical production of *cis*,*cis*-muconic acid using metabolically engineered *amycolatopsis* sp ATCC 39116, *Metab. Eng.*, 2018, **45**, 200–210.

123 C. W. Johnson, D. Salvachúa, P. Khanna, H. Smith, D. Peterson and G. Beckham, Enhancing muconic acid production from glucose and lignin-derived aromatic compounds via increased protocatechuate decarboxylase activity, *Metab. Eng. Commun.*, 2016, **3**, 111–119.

124 D. R. Vardon, M. A. Franden, C. W. Johnson, E. M. Karp, M. T. Guarnieri, J. G. Linger, M. J. Salm, T. J. Strathmann and G. T. Beckham, Correction: adipic acid production from lignin, *Energy Environ. Sci.*, 2022, **15**, 3534–3535.

125 F. Molinari, L. Pollegioni and E. Rosini, Whole-cell bioconversion of renewable biomasses-related aromatics to cis,cis-muconic acid, *ACS Sustainable Chem. Eng.*, 2023, **11**, 2476–2485.

126 J. B. J. H. van Duuren, D. Wijte, B. Karge, V. A. P. M. dos Santos, Y. Yang, A. E. Mars and G. Eggink, pH–stat fed–batch process to enhance the production of cis, cis–muconate from benzoate by pseudomonas putida KT2440-JD1, *Biotechnol. Prog.*, 2011, **28**, 85–92.

127 D. Salvachúa, C. W. Johnson, C. A. Singer, H. Rohrer, D. J. Peterson, B. A. Black, A. Knapp and G. T. Beckham, Bioprocess development for muconic acid production from aromatic compounds and lignin, *Green Chem.*, 2018, **20**, 5007–5019.

128 M. Satapathy and A. Jayapal, Biodegradation of phenol and ammonia from refinery wastewater in hybrid MBBR system by native mixed bacterial culture, *J. Environ. Eng.*, 2023, **149**, 4022087.

129 Y. Yang, Y. Zhang, C. Liu, Z. Su, R. Zhao and J. Zhou, Low-temperature phenol-degrading microbial agent: construction and mechanism, *Arch. Microbiol.*, 2023, **205**, 193.

130 P. Liu, Y. Zheng, Y. Yuan, T. Zhang, Q. Li, Q. Liang, T. Su and Q. Qi, Valorization of polyethylene terephthalate to muconic acid by engineering pseudomonas putida, *Int. J. Mol. Sci.*, 2022, **23**, 10997.

131 H. T. Kim, J. K. Kim, H. G. Cha, M. J. Kang, H. S. Lee, T. U. Khang, E. J. Yun, D.-H. Lee, B. K. Song, S. J. Park, J. C. Joo and K. H. Kim, Biological Valorization of Poly (ethylene terephthalate) Monomers for Upcycling Waste PET, *ACS Sustainable Chem. Eng.*, 2019, **7**, 19396–19406.

132 C. A. Henard, I. R. Akberdin, M. G. Kalyuzhnaya and M. T. Guarnieri, Muconic acid production from methane using rationally-engineered methanotrophic biocatalysts, *Green Chem.*, 2019, **21**, 6731–6737.
133 H. Zhang, Z. Li, B. Pereira and G. Stephanopoulos, Engineering *E. coli–E. coli* cocultures for production of muconic acid from glycerol, *Microb. Cell Fact.*, 2015, **14**, 134.
134 B. C. Saha, Hemicellulose bioconversion, *J. Ind. Microbiol. Biotechnol.*, 2003, **30**, 279–291.
135 M. M. Ishola, T. Brandberg and M. J. Taherzadeh, Simultaneous glucose and xylose utilization for improved ethanol production from lignocellulosic biomass through SSFF with encapsulated yeast, *Biomass Bioenergy*, 2015, **77**, 192–199.
136 R. Liu, L. Liang, F. Li, M. Wu, K. Chen, J. Ma, M. Jiang, P. Wei and P. Ouyang, Efficient succinic acid production from lignocellulosic biomass by simultaneous utilization of glucose and xylose in engineered *escherichia coli*, *Bioresour. Technol.*, 2013, **149**, 84–91.
137 S. R. Kim, Y.-C. Park, Y.-S. Jin and J.-H. Seo, Strain engineering of *Saccharomyces cerevisiae* for enhanced xylose metabolism, *Biotechnol. Adv.*, 2013, **31**, 851–861.
138 R. Fujiwara, S. Noda, T. Tanaka and A. Kondo, Metabolic engineering of escherichia coli for shikimate pathway derivative production from glucose–xylose co-substrate, *Nat. Commun.*, 2020, **11**, 279.
139 Y. Lin, X. Sun, Q. Yuan and Y. Yan, Extending shikimate pathway for the production of muconic acid and its precursor salicylic acid in *escherichia coli*, *Metab. Eng.*, 2014, **23**, 62–69.
140 S. Wang, M. Bilal, Y. Zong, H. Hu, W. Wang and X. Zhang, Development of a Plasmid-Free Biosynthetic Pathway for Enhanced Muconic Acid Production in Pseudomonas chlororaphis HT66, *ACS Synth. Biol.*, 2018, **7**, 1131–1142.
141 T. Dardé, É. Diomar, X. Schultze and D. Taton, An expedient route to bio-based polyacrylate alternatives with inherent post-chemical modification and degradation capabilities by organic catalysis for polymerization of muconate esters, *Angew. Chem., Int. Ed.*, 2024, **63**, e202411249.
142 Y. Zhang, Q. Lei, S. Zhang, L. Dai, B. Lyu and L. Liu, Biobased unsaturated polyester thermosets from castor oil and isosorbide with life cycle assessment, *ACS Sustainable Chem. Eng.*, 2024, **13**, 374–385.
143 A. F. Naves, H. T. C. Fernandes, A. P. S. Immich and L. H. Catalani, Enzymatic syntheses of unsaturated polyesters based on isosorbide and isomannide, *J. Polym. Sci., Part A:Polym. Chem.*, 2013, **51**, 3881–3891.
144 D. Maniar, C. Fodor, I. K. Adi, A. J. Woortman, J. van Dijken and K. Loos, Enzymatic synthesis and characterization of muconic acid–based unsaturated polymer systems, *Polym. Int.*, 2020, **70**, 555–563.
145 D. Maniar, C. Fodor, I. K. Adi, A. J. J. Woortman, J. Van Dijken and K. Loos, Enzymatic synthesis of muconic acid-based polymers: trans, trans-dimethyl muconate and trans, β-dimethyl hydromuconate, *Polymers*, 2021, **13**, 2498.
146 W. R. Hertler, T. RajanBabu, D. W. Ovenall, G. S. Reddy and D. Y. Sogah, Group transfer polymerization with polyunsaturated esters and silyl polyenolates, *J. Am. Chem. Soc.*, 1988, **110**, 5841–5853.
147 A. Wei, X. Zhao, Q. Lei, T. Zhou, S.-J. Xiong, X. Shen, J.-L. Wen and T.-Q. Yuan, Biobased unsaturated polyester adhesives from muconic acid *via* radical cross-linking for excellent multisolvent resistance, *ACS Sustainable Chem. Eng.*, 2025, **13**, 19136–19144.
148 T.-T. Lv, J. Liu, L.-J. He, H. Yuan and T.-Q. Yuan, An ultrathin and robust single-ion conducting interfacial layer for dendrite-free lithium metal batteries, *J. Energy Chem.*, 2024, **98**, 414–421.
149 T. Itoh, Y. Mitsuda, T. Ebina, T. Uno and M. Kubo, Solid polymer electrolytes composed of polyanionic lithium salts and polyethers, *J. Power Sources*, 2009, **189**, 531–535.
150 S. Kamarulzaman, Z. M. Png, E. Q. Lim, I. Z. S. Lim, Z. Li and S. S. Goh, Covalent adaptable networks from renewable resources: Crosslinked polymers for a sustainable future, *Chem*, 2023, **9**, 2771–2816.
151 J. J. Q. Mah, N. E. B. Surat'man, B. Li, S. Wang and Z. Li, Recent advances of dynamic covalent chemistry polymers aligning with principles of green chemistry, *ChemSusChem*, 2025, **18**, e202500480.
152 L. Yan, A. j. Huertas-Alonso, H. Liu, L. Dai, C. Si and M. H. Sipponen, Lignin polymerization: towards high-performance materials, *Chem. Soc. Rev.*, 2025, **54**, 6634–6651.

